

1 A monogenic and fast-responding Light-Inducible Cre recombinase as  
2 a novel optogenetic switch

3

4

5 Hélène Duplus-Bottin<sup>1</sup>, Martin Spichty<sup>1,\*</sup>, Gérard Triqueneaux<sup>1</sup>, Christophe Place<sup>2</sup>, Philippe  
6 Emmanuel Mangeot<sup>3</sup>, Théophile Ohlmann<sup>3</sup>, Franck Vittoz<sup>2</sup> and Gaël Yvert<sup>1,#</sup>

7

8

9 1) Laboratory of Biology and Modeling of the Cell, Universite de Lyon, Ecole Normale  
10 Superieure de Lyon, CNRS, UMR5239, Universite Claude Bernard Lyon 1, 46 allee d'Italie  
11 69007 Lyon, France.

12

13 2) Laboratory of Physics, Universite de Lyon, Ecole Normale Superieure de Lyon, CNRS,  
14 UMR5672, Universite Claude Bernard Lyon 1, 46 allee d'Italie 69007 Lyon, France.

15

16 3) CIRI-Centre International de Recherche en Infectiologie, Universite Claude Bernard Lyon  
17 1, Universite de Lyon, Inserm, U1111, CNRS, UMR5308, Ecole Normale Superieure de  
18 Lyon, 69007, Lyon, France

19

20 \*) Current address: Laboratoire d'Innovation Moléculaire et Applications, Site de Mulhouse –  
21 IRJBD, 3 bis rue Alfred Werner, 68057 Mulhouse Cedex, France

22

23 #) corresponding author.

24

25 Contact Information:

26 Gael Yvert

27 Laboratory of Biology and Modeling of the Cell,  
28 Ecole Normale Supérieure de Lyon, CNRS, Université de Lyon  
29 46 Allée d'Italie, Lyon, F-69007, France

30 [Gael.Yvert@ens-lyon.fr](mailto:Gael.Yvert@ens-lyon.fr)

31

32

33

34 ABSTRACT

35

36

37 Optogenetics enables genome manipulations with high spatiotemporal resolution,  
38 opening exciting possibilities for fundamental and applied biological research. Here, we  
39 report the development of LiCre, a novel light-inducible Cre recombinase. LiCre is made of a  
40 single flavin-containing protein comprising the asLOV2 photoreceptor domain of *Avena*  
41 *sativa* fused to a Cre variant carrying destabilizing mutations in its N-terminal and C-terminal  
42 domains. LiCre can be activated within minutes of illumination with blue light, without the  
43 need of additional chemicals. When compared to existing photoactivatable Cre recombinases  
44 based on two split units, LiCre displayed faster and stronger activation by light as well as a  
45 lower residual activity in the dark. LiCre was efficient both in yeast, where it allowed us to  
46 control the production of  $\beta$ -carotene with light, and in human cells. Given its simplicity and  
47 performances, LiCre is particularly suited for fundamental and biomedical research, as well as  
48 for controlling industrial bioprocesses.

49

50 INTRODUCTION  
51

52 The wealth of knowledge currently available on the molecular regulations of living  
53 systems - including humans - largely results from our ability to introduce genetic changes in  
54 model organisms. Such manipulations have been extremely informative because they can  
55 unambiguously demonstrate causal effects of molecules on phenotypes. The vast majority of  
56 these manipulations were made by first establishing a mutant individual - or line of  
57 individuals - and then studying it. This classic approach has two limitations. First, the  
58 mutation is present in all cells of the individual. This complicates the analysis of the  
59 contribution of specific cells or cell-types to the phenotypic alterations that are observed at the  
60 whole-organism level. Second, when a mutation is introduced long before the phenotypic  
61 analysis, it is possible that the organism has "adapted" to it, either via compensatory  
62 regulations or, in case of mutant lines maintained over multiple generations, by compensatory  
63 mutations.

64  
65 For these reasons, other approaches relying on site-specific recombinases were  
66 developed to introduce specific mutations in a restricted number of cells of the organism, and  
67 at a specific time. For instance, the Cre/LoxP system<sup>1,2</sup> consists of two manipulations: a stable  
68 insertion, in all cells, of foreign 34-bp DNA sequences called LoxP, and the expression of the  
69 Cre recombinase in some cells only, where it modifies the DNA by catalyzing recombination  
70 between the LoxP sites. The result is a mosaic animal - or plant, or colony of cells - where  
71 chromosomal DNA has been rearranged in some cells only. Cre is usually introduced via a  
72 transgene that is only expressed in the cells to be mutated. The location and orientation of  
73 LoxP sites can be chosen so that recombination generates either a deletion, an inversion or a  
74 translocation. Similar systems were developed based on other recombinases/recognition  
75 targets, such as Flp/FRT<sup>3</sup> or Dre-rox<sup>4</sup>. To control the timing of recombination, several  
76 systems were made inducible. Tight control was obtained using recombinases that are inactive  
77 unless a chemical ligand is provided to the cells. For example, the widely-used Cre-ERT  
78 chimeric protein can be activated by 4-hydroxy-tamoxifen<sup>5</sup>. Other inducible systems rely on  
79 chemical-induced dimerization of two halves of the recombinase. For example, the FKBP-  
80 FRB split Cre system consists of two inactive proteins that can assemble in the presence of  
81 rapamycin to form a functional recombinase complex<sup>6</sup>. Similar systems were reported that  
82 rendered dimerization of the split Cre fragments dependent on phytohormones<sup>7</sup>. Although  
83 powerful, these systems present some caveats: ligands are not always neutral to cells and can

84 therefore perturb the biological process under investigation; since they diffuse in tissues, the  
85 control of activation is sometimes not precise enough in space and/or time; and the cost or  
86 side-effects of chemical inducers can be prohibitive for industrial or biomedical applications.

87

88 More recently, several authors modified these dimerizing split recombinases to make  
89 them inducible by light instead of chemicals. This presents several advantages because i) light  
90 can be used with extreme spatiotemporal precision and high reproducibility, ii) when applied  
91 at low energy, it is neutral to many cell types, and iii) it is very cheap and therefore scalable to  
92 industrial processes. The dimerization systems that were used come from developments made  
93 in optogenetics, where various light, oxygen or voltage (LOV) protein domains have been  
94 used as photosensory modules to control transcription<sup>8</sup>, protein degradation<sup>9</sup>, dimerization<sup>10-12</sup>  
95 or subcellular relocalization<sup>13,14</sup>. LOV domains belong to the Per-Arnt-Sim (PAS)  
96 superfamily found in many sensors. They respond to light via a flavin cofactor located at their  
97 center. In the *asLOV2* domain, blue light generates a covalent bond between a carbon atom of  
98 a flavin mononucleotide (FMN) cofactor and a cystein side chain of the PAS fold<sup>15,16</sup>,  
99 resulting in a conformational change including the unfolding of a large C-terminal  $\alpha$ -helical  
100 region called the  $J\alpha$  helix<sup>17,18</sup>. Diverse optogenetics tools have been developed by fusing LOV  
101 domains to functional proteins, in ways that made the  $J\alpha$  folding/unfolding critical for  
102 activity<sup>19</sup>. Among these tools are several photodimerizers that proved useful to control the  
103 activity of recombinases. Taslimi *et al.*<sup>20</sup> reported blue-light dependent heterodimerization of  
104 a split Cre recombinase using the CIB1-CRY2 dimerizers from the plant *Arabidopsis thaliana*  
105 and others successfully used the nMag/pMag dimerizers derived from Vivid (VVD), a protein  
106 of the fungus *Neurospora crassa*<sup>21,22</sup>. A third system was based on dimerizers derived from  
107 the chromophore-binding photoreceptor phytochrome B (PhyB) of *A. thaliana* and its  
108 interacting factor PIF3. In this case, red light was used for stimulation instead of blue light,  
109 but the system required the addition of an expensive chemical, the chromophore  
110 phycocyanobilin<sup>23</sup>.

111

112 An ideal inducible recombinase is one that ensures both low basal activity and high  
113 induced activity, that is simple to implement, cheap to use and fast to induce. All dimerizing  
114 split Cre systems have in common that two protein units must be assembled in order to form  
115 one functional Cre. Thus, the probability of forming a functional recombination synapse -  
116 which normally requires four Cre molecules - is proportional to the product of the two units'  
117 cellular concentrations to the power of four. Split systems therefore strongly depend on the

118 efficient expression of their two different coding sequences, as previously reported<sup>24</sup>. An  
119 inducible system based on a single protein may avoid this limitation. Its implementation by  
120 transgenesis would also be simpler, especially in vertebrates.

121

122 We report here the development of LiCre, a novel Light-Inducible Cre recombinase  
123 that is made of a single flavin-containing protein. LiCre can be activated within minutes of  
124 illumination with blue light, without the need of additional chemicals, and it shows extremely  
125 low background activity in absence of stimulation as well as high induced activity. Using the  
126 production of carotenoids by yeast as a case example, we show that LiCre and blue light can  
127 be combined to control metabolic switches that are relevant to the problem of metabolic  
128 burden in bioprocesses. We also report that LiCre can be used efficiently in human cells,  
129 making it suitable for biomedical research. Since LiCre offers cheap and precise  
130 spatiotemporal control of a genetic switch, it is amenable to numerous biotechnological  
131 applications, even at industrial scales.

132                   RESULTS

133

134                   *The stabilizing N-ter and C-ter  $\alpha$ -helices of the Cre recombinase are critical for its*  
135                   *activity*

136

137                   A variety of optogenetic tools have been successfully developed based on LOV  
138 domain proteins, which possess  $\alpha$ -helices that change conformation in response to light<sup>25</sup>. We  
139 reasoned that fusing a LOV domain to a helical domain of Cre that is critical for its function  
140 could generate a single protein with light-dependent recombinase activity. We searched for  
141 candidate  $\alpha$ -helices by inspecting the structure of the four Cre units complexed with two LoxP  
142 DNA targets<sup>26,27</sup> (Fig. 1a-b). Each subunit folds in two domains that bind to DNA as a clamp.  
143 Guo *et al.* initially reported that helices  $\alpha$ A and  $\alpha$ E of the amino-terminal domain, as well as  
144 helix  $\alpha$ N of the C-terminal domain participate to inter-units contacts<sup>27</sup>. This role of helix  $\alpha$ N  
145 was later confirmed by Ennifar *et al*<sup>26</sup>. Contacts between  $\alpha$ A and  $\alpha$ E associate all four amino-  
146 terminal domains (Fig. 1a) and contacts involving  $\alpha$ N lock the four carboxy-terminal domains  
147 in a cyclic manner (Fig. 1b). These helices were therefore good candidates for manipulating  
148 Cre activity. We focused on  $\alpha$ A and  $\alpha$ N because their location at protein extremities was  
149 convenient to design chimeric fusions.

150

151                   We tested the functional importance of helices  $\alpha$ A and  $\alpha$ N by gradually eroding them.  
152 We evaluated the corresponding mutants by expressing them in yeast cells where an active  
153 Cre can excise a repressive DNA element flanked by LoxP sites, and thereby switch ON the  
154 expression of a Green Fluorescent Protein (GFP) (Fig. 1c). After inducing the expression of  
155 Cre mutants with galactose, we counted by flow cytometry the proportion of cells that  
156 expressed GFP and we used this measure to compare recombinase activities of the different  
157 mutants (Fig. 1d). As a control, we observed that the wild-type Cre protein activated GFP  
158 expression in all cells under these conditions. Mutants lacking the last 2 or the last 3 carboxy-  
159 terminal residues displayed full activity. In contrast, mutants lacking 4 or more of the C-ter  
160 residues were totally inactive. This was consistent with a previous observation that deletion of  
161 the last 12 residues completely suppressed activity<sup>28</sup>. Our series of mutants showed that helix  
162  $\alpha$ N is needed for activity and that its residue D341 is crucial. The role of this aspartic acid is  
163 most likely to stabilize the complex: the tetramer structure indicates salt bridges between  
164 D341 and residue R139 of the adjacent unit (Fig. 1e). Interestingly, E340 might have a similar  
165 role by interacting with R192, although this residue was not essential for activity.

166 Biomolecular simulations using a simplistic force-field model showed that the free-energy  
167 barrier for displacing the  $\alpha$ N helix was much lower if E340 and D341 were replaced by  
168 alanines (Fig. 1f). Consistent with this prediction, we observed that a double mutant E340A  
169 D341A lost ~10% of activity (Fig. 1g). This mild (but reproducible) reduction of activity  
170 suggested that the double mutation E340A D341A led to a fragilized version of Cre where  
171 multimerization was suboptimal.

172

173 We also tested the functional importance of  $\alpha$ -helix A, either in a normal context  
174 where the C-terminal part of Cre was intact or where it carried the destabilizing E340A  
175 D341A mutation (Fig. 1g). Deletion of residues 2-37, which entirely ablated helix A,  
176 eliminated enzymatic activity (Fig. 1g). Very interestingly, the effect of shorter deletions  
177 depended on the C-terminal context. When the C-terminus was wild-type, removing residues  
178 2-21 (immediately upstream of helix A) had no effect and removing residues 2-28 (partial  
179 truncation of  $\alpha$ A) decreased the activity by ~10%. When the C-terminus contained the E340A  
180 D341A mutation, deletions 2-21 and 2-28 were much more severe, reducing the activity by  
181 12% and 80%, respectively. This revealed genetic interactions between the extremities of the  
182 protein, which is fully consistent with a cooperative role of helices  $\alpha$ A and  $\alpha$ N in stabilizing  
183 an active tetramer complex. From these observations, we considered that photo-control of Cre  
184 activity might be possible by fusing  $\alpha$ A and  $\alpha$ N helices to LOV domain photoreceptors.

185

186 *Fusions of LOV domains to monogenic Cre confer light-inducible activity*

187

188 Our first strategy was to fuse the  $\alpha$ N carboxy-terminal helix of Cre to the amino-  
189 terminal cap of the LOV-domain of protein Vivid (VVD), a well-characterized photosensor  
190 from *Neurospora crassa*<sup>12,29,30</sup>. The resulting chimeric protein, which contained the full-  
191 length Cre connected to VVD via four amino-acids, did not display light-dependent  
192 recombinase activity (Supplementary Fig. S1). Our next strategy was based on a modified  
193 version of the asLOV2 domain from *Avena sativa* which had been optimized by Guntas *et*  
194 *al.*<sup>31</sup>. These authors used it to build an optogenetic dimerizer by fusing its  $J\alpha$  C-ter helix to the  
195 bacterial *SsrA* peptide. Instead, we fused  $J\alpha$  to the  $\alpha$ A amino-terminal helix of Cre. Using the  
196 same GFP reporter system as described above for detecting *in-vivo* recombination in yeast, we  
197 built a panel of constructs with various fusion positions and we directly quantified their  
198 activity with and without blue-light illumination. All fusions displayed reduced activity in  
199 both dark and light conditions as compared to wild-type Cre. Three constructs -

200 corresponding to fusions of asLOV2 to residues 19, 27 and 32 of Cre, respectively - displayed  
201 higher activity after light stimulation. We recovered the corresponding plasmids from yeast,  
202 amplified them in bacteria to verify their sequence and re-transformed them in yeast which  
203 confirmed the differential activity between dark and light conditions for all three constructs  
204 (Fig. 2a). Fusion at position 32 (named LOV2\_Cre32) displayed the highest induction by  
205 light, with activity increasing from 15% in dark condition to 50% after 30 minutes of  
206 illumination. Although this induction was significant, a 15% activity of the non-induced form  
207 remained too high for most applications. We therefore sought to reduce this residual activity,  
208 which we did in two ways.

209

210 First, we randomized the residues located at the junction between asLOV2 and Cre.  
211 We used degenerate primers and *in-vivo* recombination (see methods) to mutagenize  
212 LOV2\_Cre32 at these positions and we directly tested the activity of about 90 random clones.  
213 Five of them showed evidence of low residual activity in the dark and we characterized them  
214 further by sequencing and re-transformation. For all five clones, residual activity was indeed  
215 reduced as compared to LOV2\_Cre32, with the strongest reduction being achieved by an  
216 isoleucine insertion at the junction position (Fig. 2b iv). However, this improvement was also  
217 accompanied by a weaker induced activity and a larger variability between independent  
218 assays.

219

220 As a complementary approach to reduce residual activity, we took advantage of the  
221 above-described genetic interaction between N-ter truncations and C-ter mutations targeting  
222 residues 340 and 341. We built another series of constructs where asLOV2 fusions to  $\alpha$ A  
223 helix were combined with the A340A341 double mutation. This approach yielded one  
224 construct (LOV2\_CreAA20), corresponding to fusion at position 20, which displayed a  
225 residual activity that was undistinguishable from the negative control, and a highly-  
226 reproducible induced activity of ~25% (Fig. 2c). We called this construct LiCre (for 'Light-  
227 inducible Cre') and characterized it further.

228

229 *Efficiency and dynamics of LiCre photoactivation*

230

231 We placed LiCre under the expression of the  $P_{MET17}$  promoter and we tested various  
232 illumination intensities and durations on cells that were cultured to stationary phase in  
233 absence of methionine (full expression). Activity was very low without illumination and

234 increased with both the intensity and duration of light stimulation (Fig. 3a). The minimal  
235 intensity required for stimulation was comprised between 0.057 and 1.815 mW/cm<sup>2</sup>. The  
236 highest activity (~65% of switched cells) was obtained with 90 minutes illumination at 36.3  
237 mW/cm<sup>2</sup>. Extending illumination to 180 minutes did not further increase the fraction of  
238 switched cells. Remarkably, we observed that 2 minutes of illumination was enough to switch  
239 5% of cells, and 5 minutes illumination generated 10% of switched cells (Fig. 3b).

240

241 We compared these performances with those of two previous systems that were both  
242 based on light-dependent complementation of a split Cre enzyme. We constructed plasmids  
243 coding for proteins CreN59-nMag and pMag-CreC60 described in Kawano *et al.*<sup>21</sup> and  
244 transformed them in our yeast reporter strain. Similarly, we constructed and tested plasmids  
245 coding for the proteins CRY2<sup>L348F</sup>-CreN and CIB1-CreC described in Taslimi *et al.*<sup>20</sup>. All four  
246 coding sequences were placed under the control of the yeast PMET17 promoter. We analyzed  
247 the resulting strains as above after adapting light to match the intensity recommended by the  
248 authors (1.815 mW/cm<sup>2</sup> for nMag/pMag and 5.45 mW/cm<sup>2</sup> for CRY2<sup>L348F</sup>/CIB1). As shown  
249 in Fig. 3c, we validated the photoactivation of nMag/pMag split Cre in yeast, where activity  
250 increased about 4-fold following 90 minutes of illumination, but we were not able to observe  
251 photoactivation of the CRY2<sup>L348F</sup>/CIB1 split Cre system (Fig. 3d). In addition, the  
252 photoactivation of nMag/pMag split Cre was not as fast as the one of LiCre, since 30 minutes  
253 of illumination was needed to observe a significant increase of activity. This observation is  
254 consistent with the fact that dimerization of split Cre, which is not required for LiCre, limits  
255 the rate of formation of an active recombination synapse. Another difference was that, unlike  
256 LiCre, nMag/pMag split Cre displayed a mild but significant background activity in absence  
257 of illumination (~6% of switched cells) (Fig. 3c). Altogether, these results show that, at least  
258 in the yeast cellular context, LiCre outperforms these two other systems in terms of  
259 efficiency, rapidity and residual background activity.

260

261 To demonstrate the control of a biological activity by light, we built a reporter where  
262 Cre-mediated excision enabled the expression of the *HIS3* gene necessary for growth in  
263 absence of histidine. We cultured cells carrying this construct and expressing LiCre and we  
264 spotted them at various densities on two HIS<sup>-</sup> selective plates. One plate was illuminated  
265 during 90 minutes while the other one was kept in the dark and both plates were then  
266 incubated for growth. After three days, colonies were abundant on the plate that had been

267 illuminated and very rare on the control plate (Fig. 3e). LiCre can therefore be used to trigger  
268 cell growth with light.

269

270 We then sought to observe the switch in individual cells. To do so, we replaced GFP  
271 by mCherry in our reporter system, so that the excitation wavelength of the reporter did not  
272 overlap with stimulation of LiCre. We expressed and stimulated LiCre (90min at 3.63  
273 mW/cm<sup>2</sup>) in cells carrying this reporter and subsequently imaged them over time. As  
274 expected, we observed the progressive apparition of mCherry signal in a fraction of cells (Fig.  
275 3f-g).

276

277 Although convenient for high-throughput quantifications, reporter systems based on  
278 the *de novo* production and maturation of fluorescent proteins require a delay between the  
279 time of DNA excision and the time of acquisition. We wished to bypass this limitation and  
280 directly quantify DNA recombination. For this, we designed oligonucleotides outside of the  
281 region flanked by LoxP sites. The hybridization sites of these primers are too distant for  
282 efficient amplification of the non-edited DNA template but, after Cre-mediated excision of  
283 the internal region, these sites become proximal and PCR amplification is efficient (Fig. 3h).  
284 We mixed known amounts of edited and non-edited genomic DNA and performed real-time  
285 qPCR to build a standard curve that could be used to infer the proportion of edited DNA from  
286 qPCR signals. After this calibration, we applied this qPCR assay on genomic DNA extracted  
287 from cells collected immediately after different durations of illumination at moderate intensity  
288 (3.63 mW/cm<sup>2</sup>). Results were in full agreement with GFP-based quantifications (Fig. 3i).  
289 Excision of the target DNA occurred in a significant fraction of cells after only 2 minutes of  
290 illumination, and we estimated that excision occurred in about 30% and 40% of cells after 20  
291 and 40 minutes of illumination, respectively. To determine if DNA excision continued to  
292 occur after switching off the light, we re-incubated half of the cells for 90 minutes in the dark  
293 prior to harvest and genomic DNA extraction. The estimated frequency of DNA excision was  
294 strikingly similar to the one measured immediately after illumination (Fig. 3j). We conclude  
295 that the reversal of activated LiCre to its inactive state is very rapid in the dark (within  
296 minutes).

297

298 The qPCR assay also allowed us to compare the efficiency of light-induced  
299 recombination between cell populations in exponential growth or in stationary phase. This  
300 revealed that LiCre photoactivation was about 4-fold more efficient in non-dividing cells (Fig.

301 3k). Although the reasons for this difference remain to be determined, this increase of LiCre  
302 photoactivation at stationary phase makes it particularly suitable for bioproduction  
303 applications, where metabolic switching is often desired after the growth phase (see  
304 discussion).

305

306 *Model of LiCre photo-activation*

307

308 We built a structural model of LiCre to conceptualize its mode of activation (Fig. 4a).  
309 We based this model on i) the available structure of the Cre tetramer complexed with its target  
310 DNA<sup>27</sup>, ii) the available structure of asLOV2 in its dark state<sup>31</sup> and iii) knowledge that the J $\alpha$   
311 helix of asLOV2 domains unfolds after light activation<sup>17,18</sup>. From this model, we hypothesize  
312 that LiCre photoactivation may occur via two synergistic effects. First, the domain asLOV2  
313 likely prevents Cre tetramerization in the dark state simply because of its steric occupancy.  
314 The unfolding of the J $\alpha$  helix in the light state may allow asLOV2 to liberate the  
315 multimerizing interface. Second, because the J $\alpha$  helix of asLOV2 and the  $\alpha$ A helix of Cre are  
316 immediately adjacent, it is unlikely that both of them can fold simultaneously in their native  
317 conformation. The unfolding of J $\alpha$  in the light state may therefore stimulate proper folding of  
318  $\alpha$ A, and thereby allow  $\alpha$ A to bind to the adjacent Cre unit. Structural *in vitro* studies of LiCre  
319 itself will be needed to validate these predictions.

320

321 According to this model, there are two possible steps limiting the activation of LiCre  
322 in any one individual cell: the conformational change of LiCre monomers and the assembly of  
323 a functional recombination synapse. We sought to investigate whether one of these two steps  
324 was predominantly limiting over the other. We did this by studying cells carrying both the  
325 GFP (green) and the mCherry (red) reporters. If monomer activation is predominantly  
326 limiting, then two populations of cells are expected in an illuminated culture: cells that have  
327 activated enough LiCre molecules to form an active synapse will efficiently switch both  
328 reporters, and cells that have not activated enough LiCre monomers will leave both reporters  
329 intact and display no fluorescence. Conversely, if assembly of a functional recombination  
330 synapse is predominantly limiting, then the probability that a cell switches one reporter  
331 should be independent on what happens at the other reporter and the population will then  
332 contain a significant proportion of cells displaying fluorescence in only one color. After  
333 stimulation with 3.63 mW/cm<sup>2</sup> blue light for 180 min, one third of the cells had switched  
334 only one of the two reporters (fluorescence in only one of the channels), ruling out the

335 possibility that monomer activation is solely limiting (Fig. 4b). However, the probability that  
336 a reporter had switched depended on whether the other reporter had also switched. For  
337 example, the proportion of green cells in the whole population (marginal probability to switch  
338 the green reporter) was ~20%, but the proportion of green cells in the subpopulation of red  
339 cells (conditional probability) was over 30%. Similarly, red cells were more frequent in the  
340 subpopulation of green cells than in the whole population (Fig. 4b). These observations ruled  
341 out the possibility that formation of a functional LiCre:DNA synaptic complex was solely  
342 limiting. We conclude that neither monomer activation nor synapse formation is the sole rate-  
343 limiting step *in vivo*.

344

#### 345 *LiCre provides a light-switch for carotenoid production*

346

347 LiCre offers a way to change the activities of cells without adding any chemical to  
348 their environment. This potentially makes it an interesting tool to address the limitations of  
349 metabolic burden in industrial bioproduction (see discussion). We therefore tested the  
350 possibility to use LiCre to control the production of a commercial compound with light.

351

352 Carotenoids are pigments that can be used as vitamin A precursors, anti-oxydants or  
353 coloring agents, making them valuable for the food, agriculture and cosmetics industries<sup>32</sup>.  
354 Commercial carotenoids are generally produced by chemical synthesis or extraction from  
355 vegetables, but alternative productions based on microbial fermentations offer remarkable  
356 advantages, including the use of low-cost substrates and therefore a high potential for  
357 financial gains. Bioproduction of carotenoids from microbes has therefore received an  
358 increasing interest. It can be based on microorganisms that naturally produce carotenoids<sup>32</sup>. It  
359 is also possible to introduce recombinant biosynthesis pathways in host microorganisms,  
360 which offers the advantage of a well-known physiology of the host and of optimizations by  
361 genetic engineering. For these reasons, strategies were previously developed to produce  
362 carotenoids in the yeast *S. cerevisiae*. Expressing three enzymes (*crtE*, *crtI* and *crtYB*) from  
363 *Xanthophyllomyces dendrorhous* enabled *S. cerevisiae* to efficiently convert farnesyl  
364 pyrophosphate (FPP) into  $\beta$ -carotene<sup>33</sup>. FPP is naturally produced by *S. cerevisiae* from  
365 Acetyl-CoA and serves as an intermediate metabolite, in particular for the production of  
366 ergosterol which is essential for cellular viability (Fig. 5). Thus, and as for any bioproduction  
367 consuming a cellular resource, this design is associated with a trade-off: redirecting FPP to  $\beta$ -  
368 carotene limits its availability for ergosterol biosynthesis and therefore impairs growth; and

369 its consumption by the host cell can limit the flux towards the recombinant pathway. A  
370 promising way to deal with this trade-off would be to favor the flux towards ergosterol during  
371 biomass expansion and, after enough producer cells are obtained, to switch the demand in  
372 FPP towards  $\beta$ -carotene. We therefore explored if LiCre could offer this possibility.

373

374 First, we tested if LiCre could allow us to switch ON the exogenous production of  
375 carotenoids with light. If so, one could use it to trigger production at the desired time of a  
376 bioprocess. We constructed a *S. cerevisiae* strain expressing only two of the three enzymes  
377 required for  $\beta$ -carotene production. Expression of the third enzyme, a bifunctional phytoene  
378 synthase and lycopene cyclase, was blocked by the presence of a floxed terminator upstream  
379 of the coding sequence of the *crtYB* gene (Fig. 5b). Excision of this terminator should restore  
380 a fully-functional biosynthetic pathway. As expected, this strain formed white colonies on  
381 agar plates, but it formed orange colonies after transformation with an expression plasmid  
382 coding for Cre, indicating that  $\beta$ -carotene production was triggered (Fig. 5c). To test the  
383 possible triggering by light, we transformed this strain with a plasmid encoding LiCre and  
384 selected several transformants, which we cultured and exposed - or not - to blue light before  
385 spotting them on agar plates. The illuminated cultures became orange while the non-  
386 illuminated ones remained white. Plating a dilution of the illuminated cell suspension yielded  
387 a majority of orange colonies, indicating that LiCre triggered *crtYB* expression and  $\beta$ -carotene  
388 production in a high proportion of plated cells (Fig. 5c). We quantified bioproduction by  
389 dosing total carotenoids in cultures that had been illuminated or not. This revealed that 72  
390 hours after the light switch the intracellular concentration of carotenoids had jumped from  
391 background levels to nearly 200 $\mu$ g/g (Fig. 5d). Thus, LiCre allowed us to switch ON the  
392 production of carotenoids by yeast using blue light.

393

394 We then tested if LiCre could allow us to switch OFF with light the endogenous  
395 ergosterol pathway that competes with carotenoid production for FPP consumption. The first  
396 step of this pathway is catalysed by the Erg9p squalene synthase. Given the importance of  
397 FPP availability for the production of various compounds, strategies have been reported to  
398 control the activity of this enzyme during bioprocesses, especially in order to reduce it after  
399 biomass expansion<sup>34-36</sup>. These strategies were not based on light but derived from  
400 transcriptional switches that naturally occur upon addition of inhibitors or when specific  
401 nutrients are exhausted from the culture medium. To test if LiCre could offer a way to switch  
402 ERG9 activity with light, we modified the *ERG9* chromosomal locus and replaced the coding

403 sequence by a synthetic construct comprising a floxed sequence coding for Erg9p and  
404 containing a transcriptional terminator, followed by a sequence coding for the catalytic  
405 domain of the 3-hydroxy3-methylglutaryl coenzyme A reductase (tHMG1) (Fig. 5e). This  
406 design prepares *ERG9* for a Cre-mediated switch: before recombination, Erg9p is normally  
407 expressed; after recombination, *ERG9* is deleted and the tHMG1 sequence is expressed to  
408 foster the mevalonate pathway. Given that *ERG9* is essential for yeast viability in absence of  
409 ergosterol supplementation<sup>37</sup>, occurrence of the switch can be evaluated by measuring the  
410 fraction of viable yeast cells prior and after the induction of recombination. When doing so,  
411 we observed that expression of Cre completely abolished viability, regardless of illumination.  
412 In contrast, cultures expressing LiCre were highly susceptible to light: they were fully viable  
413 in absence of illumination and lost ~23% of viable cells after light exposure (Fig. 5f). Thus,  
414 LiCre offers the possibility to abolish the activity of the yeast squalene synthase by exposing  
415 cells to light.

416

#### 417 *LiCre switch in human cells*

418

419 Beyond yeast, LiCre may also have a large spectrum of applications on multicellular  
420 organisms. Therefore, we tested its efficiency in human cells. For this, we constructed a  
421 lentiviral vector derived from the simian immunodeficiency virus (SIV) and encoding a  
422 human-optimized version of LiCre with a nuclear localization signal fused to its N-terminus.  
423 To quantify the efficiency of this vector, we also constructed a stable reporter cell line where  
424 expression of a membrane-located mCherry fluorescent protein could be switched ON by  
425 Cre/Lox recombination. We obtained this line by Flp-mediated insertion of a single copy of  
426 the reporter construct into the genome of Flp-In™ 293 cells (Fig. 6a, see methods). Our assay  
427 consisted of producing LiCre-encoding lentiviral particle, depositing them on reporter cells  
428 for 24h, illuminating the infected cultures with blue light and, 28 hours later, observing cells  
429 by fluorescence microscopy. As shown in Fig. 6b, mCherry expression was not detected in  
430 non-infected reporter cells. In cultures that were infected but not illuminated, a few positive  
431 cells were observed. In contrast, infected cultures that had been exposed to blue light  
432 contained mostly positive cells. This demonstrated the efficiency of the vector and that LiCre  
433 was poorly active unless cells were illuminated. LiCre can therefore be used to switch genetic  
434 activities in human cells with blue light.

435

436

437                   DISCUSSION

438

439               By performing a mutational analysis of the Cre recombinase and testing the activity of  
440 various chimeric proteins involving Cre variants and LOV-domains, we have developed a  
441 novel, single-protein, light-inducible Cre recombinase (LiCre). As compared to two  
442 previously-existing systems relying on light-dependent dimerization of split Cre fragments,  
443 LiCre displayed lower background activity in the dark as well as faster and stronger activation  
444 by light. LiCre enabled us to use blue light to switch ON the production of carotenoids by  
445 yeast and to inactivate the yeast squalene synthase. Using a lentiviral vector and human  
446 reporter cells, we also showed that LiCre could be used as an optogenetic switch in  
447 mammalian systems. We discuss below the properties of LiCre as compared to previously-  
448 reported photo-activatable recombinases and the potential of LiCre for applications in the  
449 field of industrial bioproduction.

450

451               *LiCre versus other photo-activatable recombinases*

452

453               Several tools already exist for inducing site-specific recombination with light. They  
454 fall in two groups: those that require the addition of a chemical and those that are fully  
455 genetically-encoded. The first group includes the utilization of photocaged ligands instead of  
456 4-hydroxy-tamoxifen to induce the activity of Cre-ERT. This pioneering approach was  
457 successful in cultured human cells<sup>38</sup> as well as fish<sup>39</sup> and mouse<sup>40</sup>. Later, a more complex  
458 strategy was developed that directly rendered the active site of Cre photoactivatable via the  
459 incorporation of photocaged amino-acids<sup>41</sup>. In this case, cells were provided with non-natural  
460 amino-acids, such as the photocaged tyrosine ONBY, and were genetically modified in order  
461 to express three foreign entities: a specifically evolved pyrrolysyl tRNA synthetase, a  
462 pyrrolysine tRNA<sub>CUA</sub> and a mutant version of Cre where a critical amino-acid such as Y324  
463 was replaced by a TAG stop codon. The tRNA synthetase/tRNA<sub>CUA</sub> pair allowed the  
464 incorporation of the synthetic amino-acid in place of the nonsense mutation and the resulting  
465 enzyme was inactive unless it was irradiated with violet or ultraviolet light. This strategy  
466 successfully controlled recombination in cultured human cells<sup>41</sup> and zebrafish embryos<sup>42</sup>. We  
467 note that it presents several caveats: its combination of chemistry and transgenes is complex  
468 to implement, the presence of the tRNA synthetase/tRNA<sub>CUA</sub> pair can generate off-target  
469 artificial C-terminal tails in other proteins by bypassing natural stop codons, and  
470 violet/ultraviolet light can be harmful to cells. More recently, a radically-different chemical

471 approach was proposed which consisted of tethering an active TAT-Cre recombinase to  
472 hollow gold nanoshells<sup>43</sup>. When delivered to cells in culture, these particles remained trapped  
473 in intracellular endosomes. Near-infrared photostimulation triggered activity by releasing the  
474 recombinase via nanobubble generation occurring on the particle surface. A fourth system is  
475 based on the chromophore phycocyanobilin, which binds to the PhyB receptor of *A. thaliana*  
476 and makes its interaction with PIF3 dependent on red light. Photostimulation of this  
477 interaction was used to assemble split Cre units into a functional complex in yeast<sup>23</sup>. A major  
478 interest of these last two systems is to offer the possibility to use red light, which is less  
479 harmful to cells than blue or violet light and better penetrates tissues. However, all these  
480 strategies require to efficiently deliver chemicals to the target cells at the appropriate time  
481 before illumination; and their underlying chemistry can be expensive, especially for  
482 applications in the context of large volumes such as industrial bioprocesses.

483

484 Other systems, such as LiCre, do not need chemical additives because they are fully  
485 genetically-encoded. To our knowledge, there are currently three such systems. One is based  
486 on the sequestration of Cre between two large photo-cleavable domains<sup>44</sup>. The principle of  
487 light-induced protein cleavage is very interesting but its application to Cre showed important  
488 limitations: a moderate efficiency (~30% of ON cells after the switch), the dependence on a  
489 cellular inhibitory chaperone, and the need of violet light. The two other systems are the  
490 CRY2/CIB1 and nMag/pMag split Cre, where photo-inducible dimerizers bring together two  
491 halves of the Cre protein<sup>20,21</sup>. An important advantage of LiCre over these systems is that it is  
492 made of a single protein. The first benefit of this is simplicity. More efforts are needed to  
493 establish transgenic organisms expressing two open reading frames (ORFs) as compared to a  
494 single one. This is particularly true for vertebrate systems, where inserting several constructs  
495 requires additional efforts for characterizing transgene insertion sites and conducting genetic  
496 crosses. For this reason, in previous studies, the two ORFs of the split Cre system were  
497 combined in a single construct, where they were separated either by an internal ribosomal  
498 entry site or by a sequence coding a self-cleaving peptide<sup>20,21,45</sup>. Although helpful, these  
499 solutions have important limits: with an IRES, the two ORFs are not expressed at the same  
500 level; with a self-cleaving peptide, cleavage of the precursor protein can be incomplete,  
501 generating uncleaved products with unknown activity. This was the case for nMag/pMag split  
502 Cre in mammalian cells, where a non-cleaved form at ~72 kDa was reported and where  
503 targeted modifications of the cleavage sequence increased both the abundance of this non-  
504 cleaved form and the non-induced activity of the system<sup>45</sup>. The second benefit of LiCre being

505 a single protein is to avoid problems of suboptimal stoichiometry between the two protein  
506 units, which was reported as a possible issue for CRY2/CIB1 split Cre<sup>24</sup>. A third benefit is to  
507 avoid possible intra-molecular recombination between the homologous parts of the two  
508 coding sequences. Although not demonstrated, this undesired possibility was suspected for  
509 nMag/pMag split Cre because its two dimerizers derive from the same sequence<sup>45</sup>. The other  
510 advantages of LiCre are its performances. In the present study, we used a yeast-based assay to  
511 compare LiCre with split Cre systems. Unexpectedly, although we used the improved version  
512 of the CRY2/CIB1 split Cre containing the CRY2-L348F mutation<sup>20</sup>, it did not generate  
513 photo-inducible recombination in our assay. This is unlikely due to specificities of the  
514 budding yeast, such as improper protein expression or maturation, because the original  
515 authors reported activity in this organism<sup>20</sup>. We do not explain this result but it is consistent  
516 with the observations of Kawano *et al.*<sup>21</sup> who detected extremely low photoactivation of the  
517 original version of the CRY2/CIB1 split Cre, and with the observations of Morikawa *et al.*<sup>45</sup>  
518 who reported that the induced activity of the CRY2-L348F/CIB1 system was low and highly  
519 variable. In contrast, we validated the efficiency of nMag/pMag split Cre and so did other  
520 independent laboratories<sup>7,46,47,45</sup>. LiCre, however, displayed weaker residual activity than  
521 nMag/pMag split Cre in the dark. Reducing non-induced activity is essential for many  
522 applications where recombination is irreversible. Very recently, the nMag/pMag split Cre  
523 system was expressed in mice as a transgene - dubbed PA-Cre3.0 - which comprised the  
524 promoter sequence of the chicken beta actin gene (CAG) and synonymous modifications of  
525 the original self-cleaving coding sequence. The authors reported that this strategy abolished  
526 residual activity, and they attributed this improvement to a reduction of the expression level  
527 of the transgene<sup>45</sup>. It will therefore be interesting to introduce LiCre in mice with a similar  
528 expression system and compare it to PA-Cre3.0. Importantly, LiCre also displayed higher  
529 induced activity and a faster response to light as compared to nMag/pMag split Cre. This  
530 strong response probably results from its simplicity, since the activation of a single protein  
531 involves fewer steps than the activation of two units that must then dimerize to become  
532 functional. In conclusion, LiCre is simpler and more efficient than previously-existing photo-  
533 activatable recombinases.

534

### 535 *LiCre and industrial bioproduction*

536

537 With their capability to convert low-cost substrates into valuable chemicals, cultured  
538 cells have become essential actors of industrial production. However, although metabolic

539 pathways can be rewired in favor of the desired end-product, the yields of bioprocesses have  
540 remained limited by a challenging and universal phenomenon called metabolic burden. This  
541 effect corresponds to the natural trade-off between the fitness of host cells and their efficiency  
542 at producing exogenous compounds<sup>48</sup>. Loss of cellular fitness is sometimes due to viability  
543 issues - *e.g.* if the end-product is toxic to the producing cells - and sometimes simply to the  
544 fact that resources are allocated to the exogenous pathway rather than to the cellular needs.  
545 Reciprocally, satisfying the cellular demands can compromise the efficiency of exogenous  
546 pathways. In the case of carotenoids production by yeast, metabolic burden was shown to be  
547 substantial<sup>49</sup> ( $\mu_{max}$  reduced by ~12%). This growth defect presumably involves competition  
548 for FPP, which is consumed to produce carotenoids but which is also crucially needed by  
549 cells to synthesize ergosterol, a major constituent of their membranes<sup>50</sup>.

550

551 To avoid the limitations caused by metabolic burden, a desired solution is to  
552 artificially control molecular activities so that they can first be chosen to maximize biomass  
553 expansion and then be changed in favor of bioconversion. Technically, this can be achieved  
554 by adding inducers or repressors of gene expression into the cell culture, such as lactose or  
555 hormones, but these molecules are too expensive to be used at industrial scales. Current  
556 solutions therefore rely on physiological changes in gene expression that occur in host cells  
557 during the course of fermentation, especially at the end of biomass expansion<sup>51</sup>. For example,  
558 expression of human recombinant proteins under the yeast  $P_{MET17}$  promoter can be repressed  
559 by extracellular methionine during the growth phase and triggered later after methionine is  
560 consumed<sup>52,53</sup>. Although useful, such strategies relying on endogenous molecular regulations  
561 have two important caveats. Ensuring their robustness requires strict control of physiological  
562 parameters; and each strategy is specific to the host organism and fermentation conditions and  
563 is therefore not transferable. Such limitations would be alleviated if one could cheaply control  
564 an artificial and generic metabolic switch.

565

566 Using light as the inducer is attractive in this regard. It is physiologically neutral to  
567 most non-photosynthetic organisms, it is extremely cheap and it can be controlled in real-time  
568 with extreme accuracy and reproducibility. In addition, because algae are sometimes used as  
569 producers, engineers have already designed efficient ways to bring light to bioreactors of  
570 various scales<sup>54-56</sup>. Placing metabolic activities of producing cells under optogenetic control is  
571 therefore a promising perspective and several developments have been made in this direction.  
572 Using the EL222 optogenetic expression system, Zhao *et al.* applied a two-regimes yeast

573 fermentation with a continuous illumination that maintained ethanol metabolism during the  
574 growth phase, followed by light pulses stimulating isobutanol production during the  
575 bioconversion phase<sup>57</sup>. The potential of optogenetics was also illustrated by Milias-Argeitis *et*  
576 *al.* who designed a feedback control of *E. coli* growth and used it to stabilize fermentation  
577 performances against perturbations<sup>58</sup>.

578

579 We anticipate that LiCre can provide an alternative approach because it offers the  
580 possibility to induce irreversible genetic changes by a transient exposure to light. Applying  
581 light stimulation transiently on cells could be simpler to implement than continuously  
582 controlling light conditions in a bioreactor. By constructing appropriate Lox-based circuits,  
583 genetic changes can be designed beforehand to cause the desired switch of metabolic  
584 activities. The first switch that can be beneficial is the triggering of bioproduction itself. In  
585 principle, switching ON any artificially-designed bioproduction at the appropriate time after  
586 biomass expansion can avoid the cell-growth delays caused by metabolic burden. In the  
587 results above, we used carotenoids production as an example to illustrate how LiCre can be  
588 used to trigger bioproduction by transient illumination. To explore the potential gains on  
589 production yields, proof of concept experiments can now be made using LiCre in strains,  
590 media and fermentative conditions that are relevant to industrial processes.

591 The other switch that is often desired after biomass expansion is a reduction of the  
592 cellular demands for metabolites that are critical precursors of the product of interest. For  
593 example, reducing the activity of the yeast Erg9p squalene synthase is beneficial when  
594 producing terpenes - and in particular carotenoids - because more FPP becomes available for  
595 the pathway of interest. Previous efforts could reduce this activity by mutagenesis<sup>59</sup>,  
596 replacement of the native *ERG9* promoter<sup>60</sup> or destabilization of the Erg9p protein<sup>61</sup>. In  
597 addition, several laboratories were able to implement a dynamic switch of *ERG9* activity  
598 using conventional genetic rewiring. By placing expression of *ERG9* under the control of the  
599 *P<sub>MET3</sub>* promoter, Asadollahi *et al.*<sup>34</sup> and Amiri *et al.*<sup>62</sup> could repress it by adding methionine to  
600 the culture medium, thereby improving the production of sesquiterpenes and linalool,  
601 respectively. For the production of artemisinin, Paddon *et al.*<sup>63</sup> used the *P<sub>CTR3</sub>* promoter and  
602 CuSO<sub>4</sub>, a cheaper inhibitor than methionine. Other studies placed the expression of *ERG9*  
603 under the control of the *P<sub>HXT1</sub>* promoter, which is repressed when glucose becomes naturally  
604 exhausted from the medium<sup>35,36,64</sup>. In the present study, LiCre enabled us to inactivate *ERG9*  
605 by a transient illumination. Although full inactivation of *ERG9* causes cell death and is  
606 therefore not appropriate for industrial applications, our results show that it is possible to

607 change ERG9 activity at a desired time and using an external stimulus that is cheaper than  
608 inhibitors. Rather than full inactivation, other LiCre-based strategies can now be designed to  
609 switch from a full activity to a reduced and viable activity. For example, one could insert a  
610 weak *erg9* allele at another genomic locus of our *lox-ERG9-lox* strain, so that gene deletion is  
611 partially complemented after recombination.

612 Given these considerations, optogenetic switches - and LiCre in particular - may allow  
613 industries to address the issue of metabolic burden by integrating lighting devices in  
614 bioreactors and by building switchable producer cells.

615

616 In conclusion, LiCre provides a cheap, simple, low-background, highly-efficient and  
617 fast-responding way to induce site-specific recombination with light. Given that it works in  
618 both yeast and mammalian cells, it opens many perspectives from fundamental and  
619 biomedical research to industrial applications.

620

621                   METHODS

622

623           **Strains and plasmids.** Plasmids, strains and oligonucleotides used in this study are  
624 listed in Supplementary Tables S1, S2 and S3 respectively. LiCre plasmids are available from  
625 the corresponding author upon request.

626

627           **Yeast reporter systems.** We ordered the synthesis of sequence LoxLEULoxHIS  
628 (Supplementary Text S1) from GeneCust who cloned the corresponding BamHI fragment in  
629 plasmid pHO-poly-HO to produce plasmid pGY262. The  $P_{TEF}$ -loxP-KILEU2-STOP-loxP-  
630 sphIS5 construct can be excised from pGY262 by NotI digestion for integration at the yeast  
631 HO locus. This way, we integrated it in a *leu2 his3* strain, which could then switch from  
632 LEU+ his- to leu- HIS+ after Cre-mediated recombination (Fig. 4e). To construct a GFP-  
633 based reporter, we ordered the synthesis of sequence LEULoxGreen (Supplementary Text S1)  
634 from GeneCust who cloned the corresponding NheI-SacI fragment into pGY262 to obtain  
635 pGY407. We generated strain GY984 by crossing BY4726 with FYC2-6B. We transformed  
636 GY984 with the 4-Kb NotI insert of pGY407 and obtained strain GY1752. To remove the  
637 *ade2* marker, we crossed GY1752 with FYC2-6A and obtained strain GY1761. Plasmid  
638 pGY537 targeting integration at the LYS2 locus was obtained by cloning the BamHI-EcoRI  
639 fragment of pGY407 into the BamHI, EcoRI sites of pIS385. Plasmid pGY472 was produced  
640 by GeneCust who synthesized sequence LEULoxmCherry (Supplementary Text S1) and  
641 cloned the corresponding AgeI-EcoRI insert into the AgeI,EcoRI sites of pGY407. We  
642 generated GY983 by crossing BY4725 with FYC2-6A. We obtained GY2033 by  
643 transformation of FYC2-6B with a 4-Kb NotI fragment of pGY472. We obtained GY2207 by  
644 transformation of GY983 with the same 4-Kb NotI fragment of pGY472. To generate  
645 GY2206, we linearized pGY537 with NruI digestion, transformed in strain GY855 and  
646 selected a LEU+ Lys- colony (pop-in), which we re-streaked on 5-FoA plates for vector  
647 excision by counter-selection of URA3 (pop-out)<sup>65</sup>. Strain GY2214 was a diploid that we  
648 obtained by mating GY2206 with GY2207.

649

650           **Yeast expression plasmids.** Mutations E340A D341A were introduced by GeneCust  
651 by site-directed mutagenesis of pSH63, yielding plasmid pGY372. We generated the N-  
652 ter $\Delta$ 21 mutant of Cre by PCR amplification of the  $P_{GAL1}$  promoter of pSH63 using primer  
653 1L80 (forward) and mutagenic primer 1L71 (reverse), digestion of pSH63 by AgeI and co-  
654 transformation of this truncated plasmid and amplicon in a *trp1Δ63* yeast strain for

655 homologous recombination and plasmid rescue. We combined the N-ter $\Delta$ 21 and the C-ter  
656 E340A D341A mutations similarly, but with pGY372 instead of pSH63. We generated N-  
657 ter $\Delta$ 28 and N-ter $\Delta$ 37 mutants, combined or not with C-ter E340A D341A mutations, by the  
658 same procedure where we changed 1L71 by mutagenic primers 1L72 and 1L73, respectively.

659 To generate a Cre-VVD fusion, we designed sequence CreCVII (Supplementary Text  
660 S1) where the Cre sequence from GENBANK AAG34515.1 was fused to the VVD-  
661 M135IM165I sequence from Zoltowski *et al.*<sup>29</sup> via four additional residues (GGSG). We  
662 ordered its synthesis from GeneCust, and we co-transformed it in yeast with pSH63  
663 (previously digested by NdeI and SalI) for homologous recombination and plasmid rescue.  
664 This generated pGY286. We then noticed an unfortunate error in AAG34515.1, which reads a  
665 threonine instead of an asparagine at position 327. We cured this mutation from pGY286 by  
666 site-directed mutagenesis using primers 1J47 and 1J48, which generated pGY339 which  
667 codes for Cre-VVD described in Supplementary Fig. S1. We constructed mutant C-ter $\Delta$ 14 of  
668 Cre by site-directed mutagenesis of pGY286 using primers 1J49 and 1J50 which  
669 simultaneously cured the N327T mutation and introduced an early stop codon. Mutants C-  
670 ter $\Delta$ 2, C-ter $\Delta$ 4, C-ter $\Delta$ 6, C-ter $\Delta$ 8, C-ter $\Delta$ 10, C-ter $\Delta$ 12 of Cre were constructed by GeneCust  
671 who introduced early stop codons in pGY339 by site-directed mutagenesis.

672

673 To test LOV2\_Cre fusions, we first designed sequence EcoRI-LovCre\_chimJa-BstBI  
674 (Supplementary Text S1) corresponding to the fusion of asLOV2 with Cre via an artificial  $\alpha$ -  
675 helix. This helix was partly identical to the  $J\alpha$  helix of asLOV2 and partly identical to the  $\alpha A$   
676 helix of Cre. This sequence was synthesized and cloned in the EcoRI and BstBI sites of  
677 pSH63 by GeneCust, yielding pGY408. We then generated and directly tested a variety of  
678 LOV2\_Cre fusions. To do so, we digested pGY408 with BsiWI and MfeI and used this  
679 fragment as a recipient vector; we amplified the Cre sequence from pSH63 using primer  
680 1G42 as the reverse primer, and one of primers 1M42 to 1M53 as the forward primer (each  
681 primer corresponding to a different fusion position); we co-transformed the resulting  
682 amplicon and the recipient vector in strain GY1761, isolated independent transformants and  
683 assayed them with the protocol of photoactivation and flow-cytometry described below. We  
684 generated and tested a variety of LOV2\_CreAA fusions by following the same procedure  
685 where plasmid pGY372 was used as the PCR template instead of pSH63. A transformant  
686 corresponding to LOV2\_Cre32 and showing light-dependent activity was chosen for plasmid  
687 rescue, yielding plasmid pGY415. A transformant corresponding to LOV2\_CreAA20 was  
688 chosen for plasmid rescue, yielding plasmid pGY416. Sanger sequencing revealed that the

689 fusion sequence present in pGY416 was QID instead of QIA at the peptide junction (position  
690 149 on LiCre sequence of Supplementary Text S2). All further experiments on LiCre were  
691 derived from the fusion protein coded by pGY416.

692

693 To introduce random residues at the peptide junction of LOV2\_Cre32 (Fig. 2b), we  
694 first generated pGY417 using the same procedure as for the generation of pGY415 but with  
695 pSH47 instead of pSH63 as the PCR template so that pGY417 has a URA3 marker instead of  
696 TRP1. We then ordered primers 1N24, 1N25 and 1N26 containing degenerate sequences, we  
697 used them with primer 1F14 to amplify the Cre sequence of pSH63, we co-transformed in  
698 strain GY1761 the resulting amplicons together with a recipient vector made by digesting  
699 plasmid pGY417 with NcoI and BsiWI, and we isolated and directly tested individual  
700 transformants with the protocol of photoactivation and flow-cytometry described below.  
701 Plasmids from transformants showing evidence of reduced background were rescued from  
702 yeast and sequenced, yielding pGY459 to pGY464.

703

704 To replace the *P<sub>GAL1</sub>* promoter of pGY416 by the *P<sub>MET17</sub>* promoter, we digested it with  
705 SacI and SpeI, we PCR-amplified the *P<sub>MET17</sub>* promoter of plasmid pGY8 with primers 1N95  
706 and 1N96, and we co-transformed the two products in yeast for homologous recombination,  
707 yielding plasmid pGY466. We changed the promoter of pGY415 using exactly the same  
708 procedure, yielding plasmid pGY465. We changed the promoter of pSH63 similarly, using  
709 primer 1O83 instead of 1N96, yielding plasmid pGY502.

710

711 To express the nMag/pMag split Cre system in yeast, we designed sequence CreN-  
712 nMag-NLS-T2A-NLS-pMag-CreCpartly (Supplementary Text S1) and ordered its synthesis  
713 from GeneCust. The corresponding BglII fragment was co-transformed in yeast for  
714 homologous recombination with pGY465 previously digested with BamHI (to remove  
715 asLOV2 and part of Cre), yielding plasmid pGY488 that contained the full system. We then  
716 derived two plasmids from pGY488, each one containing one half of the split system under  
717 the control of the Met17 promoter. We obtained the first plasmid (pGY491, carrying the  
718 TRP1 selection marker) by digestion of pGY488 with SfoI and SacII and co-transformation of  
719 the resulting recipient vector with a PCR product amplified from pGY465 using primers  
720 1O80 and 1O82. We obtained the second plasmid (pGY501, carrying the URA3 selection  
721 marker) in two steps. We first removed the pMag-CreC part of pGY488 by digestion with  
722 NdeI and SacII followed by Klenow fill-in and religation. We then changed the selection

723 marker by digestion with PfoI and KpnI and co-transformation in yeast with a PCR product  
724 amplified from pSH47 with primers 1O77 and 1O89.

725

726 To express the CRY2<sup>L348F</sup>/CIB1 split Cre system in yeast, we designed sequences  
727 CIB1CreCter and CRY2CreNter and ordered their synthesis from GeneCust, obtaining  
728 plasmids pGY526 and pGY527, respectively. To obtain pGY531, we extracted the synthetic  
729 insert of pGY527 by digestion with BglII and we co-transformed it in yeast with the NdeI-  
730 BamHI fragment of pGY466 for homologous recombination. To obtain pGY532, we  
731 extracted the synthetic insert of pGY526 by digestion with BglII and we co-transformed it in  
732 yeast with the SacI-BamHI fragment of pSH47 for homologous recombination.

733

734 To build a switchable strain for carotene production, we modified EUROSCARF  
735 strain Y41388 by integrating a LoxP-KILEU2-T<sub>ADH1</sub>-LoxP cassette immediately upstream the  
736 CrtYB coding sequence of the chromosomally-integrated expression cassette described by  
737 Verwaal *et al.*<sup>33</sup>. This insertion was obtained by transforming Y41388 with a 6.6Kb BstBI  
738 fragment from plasmid pGY559 and selecting a Leu<sup>+</sup> transformant, yielding strain GY2247.  
739 To obtain pGY559, we first deleted the crtE and crtI genes from YEplac195-YB\_E\_I<sup>33</sup> by  
740 MluI digestion and religation. We then linearized the resulting plasmid with SpeI and co-  
741 transformed it for recombination in a *leu2Δ* yeast strain with a PCR amplicon obtained with  
742 primers 1P74 and 1P75 and template pGY407. After Leu<sup>+</sup> selection, the plasmid was  
743 recovered from yeast, amplified in bacteria and verified by restriction digestion and  
744 sequencing.

745

746 We used CRISPR/Cas9 to build a switchable strain for squalene synthase. We cloned  
747 the synthetic sequence gERG9 (Supplementary Text S1) in the BamHI-NheI sites of the  
748 pML104 plasmid<sup>66</sup> so that the resulting plasmid (pGY553) coded for a gRNA sequence  
749 targeting *ERG9*. This plasmid was transformed in GY2226 together with a repair-template  
750 corresponding to a 4.2-Kb EcoRI fragment of pGY547 that contained LoxP-synERG9-T<sub>ADH1</sub>-  
751 LoxP with homologous flanking sequences. The resulting strain was then crossed with  
752 Y41388 to obtain GY2236.

753

754 **Yeast culture media.** We used synthetic (S) media made of 6.7 g/L Difco Yeast  
755 Nitrogen Base without Amino Acids and 2 g/L of a powder which was previously prepared by  
756 mixing the following amino-acids and nucleotides: 1 g of Adenine, 2 g of Uracil, 2 g of

757 Alanine, 2 g of Arginine, 2 g of Aspartate, 2 g of Asparagine, 2 g of Cysteine, 2 g of  
758 Glutamate, 2 g of Glutamine, 2 g of Glycine, 2 g of Histidine, 2 g of Isoleucine, 4 g of  
759 Leucine, 2 g of Lysine, 2 g of Methionine, 2 g of Phenylalanine, 2 g of Proline, 2 g of Serine,  
760 2 g of Threonine, 2 g of Tryptophane, 2 g of Tyrosine and 2 g of Valine. For growth in  
761 glucose condition, the medium (SD) also contained 20 g/L of D-glucose. For growth in  
762 galactose condition (induction of  $P_{GAL1}$  promoter), we added 2% final (20 g/L) raffinose and  
763 2% final (20 g/L) galactose (SGalRaff medium). Media were adjusted to pH=5.8 by addition  
764 of NaOH 1N before autoclaving at 0.5 Bar. For auxotrophic selections or  $P_{MET17}$  induction,  
765 we used media where one or more of the amino-acids or nucleotides were omitted when  
766 preparing S. For example, SD-W-M was made as SD but without any tryptophane or  
767 methionine in the mix powder.

768

#### 769 **Photoactivation and flow-cytometry quantification of recombinase activity.**

770 Unless mentioned otherwise, quantitative tests were done by flow-cytometry using yeast  
771 reporter strain GY1761. For photoactivation, we used a PAUL apparatus from GenIUL  
772 equipped with 460 nm blue LEDs. Using a NovaII photometer (Ophir<sup>®</sup> Photonics), we  
773 measured that a 100% intensity on this apparatus corresponded to an energy of 36.3 mW/cm<sup>2</sup>.  
774 We used Zomei ND filters when we needed to obtain intensities that were not tunable on the  
775 device. The yeast reporter strain was transformed with the plasmid of interest, pre-cultured  
776 overnight in selective medium corresponding to conditions of transcriptional activation of the  
777 plasmid-borne Cre construct (SGalRaff-W for  $P_{GAL1}$  plasmids, SD-W-M for  $P_{MET17}$  plasmids,  
778 SD-W-U-M for split Cre systems) with no particular protection against ambient light. The  
779 saturated culture was transferred to two 96-well polystyrene flat-bottom Falcon<sup>®</sup> sterile plates  
780 (100 µl per well) and one plate was illuminated at the indicated intensities while the other  
781 plate was kept in the dark. After the indicated duration of illumination, cells from the two  
782 plates were transferred to a fresh medium allowing expression of GFP but not cell division  
783 (SD-W-H or SD-W-U-H, strain GY1761 being auxotroph for histidine) and these cultures  
784 were incubated at 30°C for 90 minutes. Cells were then either analyzed immediately by flow  
785 cytometry, or blocked in PBS + 1mM sodium azide and analyzed the following day.

786 We acquired data for 10,000 events per sample using a FACSCalibur (BD  
787 Biosciences) or a MACSQuant VYB (Miltenyi Biotech) cytometer, after adjusting the  
788 concentration of cells in PBS. We analyzed raw data files in the R statistical environment  
789 ([www.r-project.org](http://www.r-project.org)) using custom-made scripts based on the flowCore package<sup>70</sup> from  
790 bioconductor ([www.bioconductor.org](http://www.bioconductor.org)). We gated cells automatically by computing a

791 perimeter of (FSC-H, SSC-H) values that contained 40% of events (using 2D-kernel density  
792 distributions). A threshold of fluorescent intensity (GFP or mCherry) was set to distinguish  
793 ON and OFF cells (*i.e.* expressing or not the reporter). To do this, we included in every  
794 experiment a negative control made of the reporter strain transformed with an empty vector,  
795 and we chose the 99.9<sup>th</sup> percentile of the corresponding 4,000 fluorescent values (gated cells)  
796 as the threshold.

797

798 **Quantification of fluorescence levels from microscopy images.** For Fig. 3g, we  
799 segmented individual cells on bright field images using the ImageJ Lasso plugin. Then, we  
800 measured on the fluorescence images the mean gray value of pixels in each segmented area,  
801 providing single-cell measures of fluorescence. For each image, the background fluorescence  
802 level was quantified from eight random regions outside of cells and with areas similar to  
803 single cells. This background level was subtracted from the fluorescence level of each cell.

804

805 **Quantification of carotenoids from yeast.** We strictly followed the procedure  
806 described in Verwaal *et al.*<sup>33</sup>, which consists of mechanical cell lysis using glass beads,  
807 addition of pyrogallol, KOH-based saponification, and extraction of carotenoids in hexane.  
808 Quantification was estimated by optical absorption at 449 nm using a Biowave  
809 spectrophotometer.

810

811 **Human reporter cell line.** We built a reporter construct for Cre-mediated  
812 recombination in human cells based on Addgene's plasmids 55779, containing a membrane-  
813 addressed mCherry sequence<sup>67</sup> (mCherry-Mem) and 51269, containing a zsGreen-based  
814 reporter of Cre recombination<sup>68</sup>. Re-sequencing revealed that 51269 did not contain three  
815 terminator sequences but only one between the LoxP sites. We applied a multi-steps  
816 procedure to i) restore three terminators, ii) replace zsGreen with mCherry-Mem and iii) have  
817 the final reporter in a vector suitable for targeted single-site insertion. First, we inserted a  
818 LoxP site between restriction sites NheI and HindIII of pCDNA5/FRT (Invitrogen) by  
819 annealing oligonucleotides 1O98 and 1O99, digesting and cloning this adaptor with NheI and  
820 HindIII, which yielded plasmid pGY519. Second, we replaced in two different ways the  
821 zsGreen sequence of 51269 by the mCherry-Mem sequence of 55779: either by cloning a  
822 SmaI-NotI insert from 55779 into EcoRV-NotI of 51269, yielding plasmid pGY520, or by  
823 cloning a EcoRI-NotI from 55779 into EcoRI-NotI of 51269, yielding plasmid pGY521.  
824 Third, we inserted the HindIII-NotI cassette of pGY520 into the HindIII-NotI sites of

825 pGY519, yielding plasmid pGY523. Fourth, we inserted the HindIII-NotI cassette of pGY521  
826 into the HindIII-NotI sites of pGY519, yielding plasmid pGY524. Fifth, a HindIII-BamHI  
827 fragment of pGY523 containing one terminator, and a BglII-EcoRI fragment of pGY524  
828 containing another terminator were simultaneously cloned as consecutive inserts in the BglII-  
829 EcoRI sites of 51269. Finally, the resulting plasmid was digested with HindIII and BamHI to  
830 produce a fragment that was cloned into the HindIII-BglII sites of pGY524 to produce  
831 pGY525.

832 To establish stable cell lines, Flp-In™ T-REx™ 293 cells were purchased from  
833 Invitrogen (ThermoFisher) and transfected with both the Flp recombinase vector (pOG44,  
834 Invitrogen) and pGY525. Selection of clonal cells was first performed in medium containing  
835 300 µg hygromycin (Sigma). After two weeks, we identified foci of cell clusters, which we  
836 individualized by transferring them to fresh wells. One of these clones was cultured for three  
837 additional weeks with high concentrations of hygromycin (up to 400 µg) to remove  
838 potentially contaminating negative cells. The resulting cell line was named T4-2PURE.  
839

840 **Lentivirus construct and production.** A synthetic sequence was ordered from  
841 Genecust and cloned in the HindIII-NotI sites of pCDNA3.1 (Invitrogen™ V79020). This  
842 insert contained an unrelated additional sequence that we removed by digestion with BamHI  
843 and XbaI followed by blunt-ending with Klenow fill-in. The resulting plasmid (pGY561)  
844 encoded LiCre optimized for mammalian codon usage, in-frame with a N-ter located SV40-  
845 NLS signal. This NLS-LiCre sequence was amplified from pGY561 using primers Sauci and  
846 Flard (Table S3), and the resulting amplicon was cloned in the AgeI-HindIII sites of the  
847 GAE0 Self-Inactivating Vector<sup>69</sup>, yielding pGY577. Lentiviral particles were produced in  
848 Gesicle Producer 293T cells (TAKARA ref 632617) transiently transfected by pGY577 (40%  
849 of total DNA), an HIV-1 helper plasmid (45% of total DNA) and a plasmid encoding the  
850 VSV-g envelope (15%) as previously described<sup>69</sup>. Particle-containing supernatants were  
851 clarified, filtered through a 0.45-µm membrane and concentrated by ultracentrifugation at  
852 40,000 g before resuspension in 1xPBS (100 fold concentration).  
853

854 **LiCre assay in human cells.** About 3x10<sup>5</sup> cells of cell line T4-2PURE were plated in  
855 two 6-well plates. After 24 h, 100 µl of viral particules were added to each well. After another  
856 24 h, one plate was illuminated with blue-light (460 nm) using the PAUL apparatus installed  
857 in a 37°C incubator, while the other plate was kept in the dark. For illumination, we applied a  
858 sequence of 20 min ON, 20 min OFF under CO<sub>2</sub> atmosphere, 20 min ON where ON

859 corresponded to 3.63 mW/cm<sup>2</sup> illumination. Plates were then returned to the incubator and,  
860 after 28 hours, were imaged on an Axiovert135 inverted fluorescent microscope.

861

862 **Calculation of potential mean force (PMF).** We calculated the free-energy profile  
863 (reported in Figure 1f) for the unbinding of the C-terminal  $\alpha$ -helix in the tetrameric Cre-  
864 recombinase complex<sup>26</sup> (PDB Entry 1NZB) as follows. The software we used were: the  
865 CHARMM-GUI server<sup>71</sup> to generate initial input files; CHARMM version c39b1<sup>72</sup> to setup  
866 the structural models and subsequent umbrella sampling by molecular dynamics; WHAM,  
867 version 2.0.9 (<http://membrane.urmc.rochester.edu/content/wham/>) to extract the PMF; and  
868 VMD, version 1.9.2<sup>73</sup> to visualize structures. To achieve sufficient sampling by molecular  
869 dynamics, we worked with a structurally reduced model system. We focused thereby only on  
870 the unbinding of the C-terminal  $\alpha$ -helix of subunit A (residues 334:340) from subunit F.  
871 Residues that did not have at least one atom within 25 Å from residues 333 to 343 of subunit  
872 A were removed including the DNA fragments. Residues with at least one atom within 10 Å  
873 were allowed to move freely in the following simulations; the remaining residues were fixed  
874 to their positions in the crystal structure. For the calculation of the double mutant A340A341  
875 the corresponding residues were replaced by alanine residues. The systems were simulated  
876 with the CHARMM22 force field (GBSW & CMAP parameter file) and the implicit solvation  
877 model FACTS<sup>74</sup> with recommended settings for param22 (*i.e.*, cutoff of 12 Å for nonbonded  
878 interactions). Langevin dynamics were carried out with an integration time-step of 2 fs and a  
879 friction coefficient of 4 ps<sup>-1</sup> for non-hydrogen atoms. The temperature of the heat bath was set  
880 to 310 K. The hydrogen bonds were constrained to their parameter values with SHAKE<sup>75</sup>.

881 The PMF was calculated for the distance between the center of mass of the  $\alpha$ -helix  
882 (residues 334:340 of subunit A) and the center of mass of its environment (all residues that  
883 have at least one atom within 5 Å of this helix). Umbrella sampling<sup>76</sup> was performed with 13  
884 independent molecular dynamics simulations where the system was restrained to different  
885 values of the reaction coordinate (equally spaced from 4 to 10 Å) using a harmonic biasing  
886 potential with a spring constant of 20 kcal mol<sup>-1</sup> Å<sup>-1</sup> (GEO/MMFP module of CHARMM).  
887 Note that this module uses a pre-factor of  $\frac{1}{2}$  for the harmonic potential (as in the case of the  
888 program WHAM).

889 For each simulation the value of the reaction coordinate was saved at every time-step  
890 for 30 ns. After an equilibration phase of 5ns, we calculated for blocks of 5 ns the PMF and  
891 the probability distribution function along the reaction coordinate using the weighted

histogram analysis method<sup>77</sup>. A total of 13 bins were used with lower and upper boundaries at 3.75 and 10.25 Å, respectively, and a convergence tolerance of 0.01 kcal/mol. Finally, we determined for each bin its relative free energy  $F_i = -kT \ln(\bar{p}_i)$  where  $k$  was the Boltzmann constant,  $T$  the temperature (310 K) and  $\bar{p}_i$  the mean value of the probability of bin  $i$  when averaged over the five blocks. The error in the  $F_i$  estimate was calculated with  $\sigma_{F_i} = kT \sigma_{\bar{p}_i}/\bar{p}_i$  where  $\sigma_{\bar{p}_i}$  was twice the standard error of the mean of the probability. An offset was applied to the final PMF so that its lowest value was located at zero.

899

**qPCR quantification of recombinase activity.** We grew ten colonies of strain GY1761 carrying plasmid pGY466 overnight at 30°C in SD-L-W-M liquid cultures. The following day, we used these starter cultures to inoculate 12 ml of SD-W-M medium at OD<sub>600</sub> = 0.2. When monitoring growth by optical density measurements, we observed that it was fully exponential after 4 hours and until at least 8.5 hours. At 6.5 hours of growth, for each culture, we dispensed 0.1 ml in 96-well plate duplicates using one column (8 wells) per colony, we stored aliquots by centrifuging 1 ml of the cell suspension at 3300 g and freezing the cell pellet at -20°C ('Exponential' negative control) and we re-incubated the remaining of the culture at 30°C for later analysis at stationary phase. We exposed one plate (Fig. 4j 'Exponential' cyan samples) to blue light (PAUL apparatus, 460 nm, 3.63 mW/cm<sup>2</sup> intensity) for 40 min while the replicate plate was kept in the dark (Fig. 4j 'Exponential' grey samples). We pooled cells of the same column and stored them by centrifugation and freezing as above. The following day, we collected 1 ml of each saturated, froze and stored cells as above ('Stationary' negative control). We dispensed the remaining of the cultures in a series of 96-well plates (0.1 ml/well, two columns per colony) and we exposed these plates to blue light (PAUL apparatus, 460 nm, 3.63 mW/cm<sup>2</sup> intensity) for the indicated time (0, 2, 5, 10, 20 or 40 min). For each plate, following illumination, we collected and froze cells from 6 columns (Fig. 4h samples) and we reincubated the plate in the dark for 90 min before collecting and freezing the remaining 6 columns (Fig. 4i, x-axis samples). For genomic DNA extraction, we pooled cells from 6 wells of the same colony (1 column), we centrifuged and resuspended them in 280 µl in 50 mM EDTA, we added 20 µl of a 2 mg/ml Zymolyase stock solution (SEIKAGAKU, 20 U/mg) to the cell suspension and incubated it for 1h at 37°C for cell wall digestion. We then processed the digested cells with the Wizard Genomic DNA Purification Kit from Promega. We quantified DNA on a Nanodrop spectrophotometer and used ~100,000 copies of genomic DNA as template for qPCR, with primers 1P57 and 1P58 to amplify the

925 edited target and with primers 1B12, 1C22 to amplify a control HMLalpha region that we  
926 used for normalization. We ran these reactions on a Rotorgene thermocycler (Qiagen). This  
927 allowed us to quantify the rate of excision of the floxed region as  $N_{\text{Lox}} / N_{\text{Total}}$ , where  $N_{\text{Lox}}$   
928 was the number of edited molecules and  $N_{\text{Total}}$  the total number of DNA template molecules.  
929 To estimate  $N_{\text{Lox}}$ , we prepared mixtures of edited and non-edited genomic DNAs, at known  
930 ratios of 0%, 0.5%, 1%, 5%, 10%, 50%, 70%, 90%, 100% and we applied (1P57,1P58) qPCR  
931 using these mixtures as templates. This provided us with a standard curve that we then used to  
932 convert Ct values of the samples of interest into  $N_{\text{Lox}}$  values. To estimate  $N_{\text{Total}}$ , we qPCR-  
933 amplified the HMLalpha control region from templates made of increasing concentrations of  
934 genomic DNA. We then used the corresponding standard curve to convert the Ct value of  
935 HMLalpha amplification obtained from the samples of interest into  $N_{\text{Total}}$  values.

936

937

938 **ACKNOWLEDGEMENTS**

939

940 We thank Fabien Duveau for critical reading of the manuscript and for signal  
941 quantifications from microscopy images, Grégory Batt for fruitful discussions, Maria Teresa  
942 Texeira for strains, Sandrine Mouradian, Véronique Barateau and SFR Biosciences Gerland-  
943 Lyon Sud (UMS344/US8) for access to flow cytometers and technical assistance, and  
944 developers of R, Bioconductor, VMD and Ubuntu for their software. This work was  
945 supported by the European Research Council under the European Union's Seventh  
946 Framework Programme FP7/2007-2013 Grant Agreement n°281359.

947

948 **AUTHORS CONTRIBUTIONS**

949

950 Constructed plasmids and strains, performed flow cytometry and yeast experiments:  
951 H.D-B.

952 Performed qPCR and human cell experiments: G.T.

953 Performed PMF computations: M.S.

956 Wrote the paper: GY.

957 Contributed material: C.P., F.V., T.O.

958

959 COMPETING INTERESTS

960

961 The authors declare the following competing interest: A patent application covering

962 LiCre and its potential applications has been filed. Patent applicant: CNRS; inventors: Hélène

963 Duplus-Bottin, Martin Spichty and Gaël Yvert.

964

965 REFERENCES

966

967 1. Duyne, G. D. V. Cre Recombinase. *Microbiol. Spectr.* **3**, (2015).

968 2. Rajewsky, K. *et al.* Conditional gene targeting. *J. Clin. Invest.* **98**, 600–603 (1996).

969 3. Lee, T. & Luo, L. Mosaic analysis with a repressible cell marker (MARCM) for

970 *Drosophila* neural development. *Trends Neurosci.* **24**, 251–254 (2001).

971 4. Anastassiadis, K. *et al.* Dre recombinase, like Cre, is a highly efficient site-specific

972 recombinase in *E. coli*, mammalian cells and mice. *Dis. Model. Mech.* **2**, 508–515 (2009).

973 5. Feil, R. *et al.* Ligand-activated site-specific recombination in mice. *Proc. Natl. Acad.*

974 *Sci.* **93**, 10887–10890 (1996).

975 6. Jullien, N., Sampieri, F., Enjalbert, A. & Herman, J. P. Regulation of Cre recombinase

976 by ligand-induced complementation of inactive fragments. *Nucleic Acids Res.* **31**, e131–e131

977 (2003).

978 7. Weinberg, B. H. *et al.* High-performance chemical- and light-inducible recombinases

979 in mammalian cells and mice. *Nat. Commun.* **10**, 4845 (2019).

980 8. de Mena, L., Rizk, P. & Rincon-Limas, D. E. Bringing Light to Transcription: The

981 Optogenetics Repertoire. *Front. Genet.* **9**, (2018).

982 9. Renicke, C., Schuster, D., Usherenko, S., Essen, L.-O. & Taxis, C. A LOV2 Domain-

983 Based Optogenetic Tool to Control Protein Degradation and Cellular Function. *Chem. Biol.*

984 **20**, 619–626 (2013).

985 10. Kennedy, M. J. *et al.* Rapid blue-light-mediated induction of protein interactions in

986 living cells. *Nat. Methods* **7**, 973–975 (2010).

987 11. Strickland, D. *et al.* TULIPs: tunable, light-controlled interacting protein tags for cell

988 biology. *Nat. Methods* **9**, 379–384 (2012).

989 12. Nihongaki, Y., Suzuki, H., Kawano, F. & Sato, M. Genetically Engineered

990 Photoinducible Homodimerization System with Improved Dimer-Forming Efficiency. *ACS*

991 *Chem. Biol.* **9**, 617–621 (2014).

992 13. Niopek, D. *et al.* Engineering light-inducible nuclear localization signals for precise

993 spatiotemporal control of protein dynamics in living cells. *Nat. Commun.* **5**, 1–11 (2014).

994 14. Witte, K., Strickland, D. & Glotzer, M. Cell cycle entry triggers a switch between two

995 modes of Cdc42 activation during yeast polarization. *eLife* **6**, e26722 (2017).

996 15. Crosson, S. & Moffat, K. Structure of a flavin-binding plant photoreceptor domain:

997 Insights into light-mediated signal transduction. *Proc. Natl. Acad. Sci.* **98**, 2995–3000 (2001).

998 16. Swartz, T. E. *et al.* The Photocycle of a Flavin-binding Domain of the Blue Light

999 Photoreceptor Phototropin. *J. Biol. Chem.* **276**, 36493–36500 (2001).

1000 17. Swartz, T. E., Wenzel, P. J., Corchnoy, S. B., Briggs, W. R. & Bogomolni, R. A.

1001 Vibration Spectroscopy Reveals Light-Induced Chromophore and Protein Structural Changes

1002 in the LOV2 Domain of the Plant Blue-Light Receptor Phototropin 1. *Biochemistry* **41**, 7183–

1003 7189 (2002).

1004 18. Harper, S. M., Neil, L. C. & Gardner, K. H. Structural Basis of a Phototropin Light

1005 Switch. *Science* **301**, 1541–1544 (2003).

1006 19. Pudasaini, A., El-Arab, K. K. & Zoltowski, B. D. LOV-based optogenetic devices:

1007 light-driven modules to impart photoregulated control of cellular signaling. *Front. Mol.*

1008 *Biosci.* **2**, (2015).

1009 20. Taslimi, A. *et al.* Optimized second-generation CRY2-CIB dimerizers and

1010 photoactivatable Cre recombinase. *Nat. Chem. Biol.* **12**, 425–430 (2016).

1011 21. Kawano, F., Okazaki, R., Yazawa, M. & Sato, M. A photoactivatable Cre-loxP

1012 recombination system for optogenetic genome engineering. *Nat. Chem. Biol.* **12**, 1059–1064

1013 (2016).

1014 22. Sheets, M. B., Wong, W. W. & Dunlop, M. J. Light-Inducible Recombinases for  
1015 Bacterial Optogenetics. *ACS Synth. Biol.* **9**, 227–235 (2020).

1016 23. Hochrein, L., Mitchell, L. A., Schulz, K., Messerschmidt, K. & Mueller-Roeber, B. L-  
1017 SCRaMbLE as a tool for light-controlled Cre-mediated recombination in yeast. *Nat.*  
1018 *Commun.* **9**, 1931 (2018).

1019 24. Meador, K. *et al.* Achieving tight control of a photoactivatable Cre recombinase gene  
1020 switch: new design strategies and functional characterization in mammalian cells and rodent.  
1021 *Nucleic Acids Res.* **47**, e97–e97 (2019).

1022 25. Weitzman, M. & Hahn, K. M. Optogenetic approaches to cell migration and beyond.  
1023 *Curr. Opin. Cell Biol.* **30**, 112–120 (2014).

1024 26. Ennifar, E., Meyer, J. E. W., Buchholz, F., Stewart, A. F. & Suck, D. Crystal structure  
1025 of a wild-type Cre recombinase–loxP synapse reveals a novel spacer conformation suggesting  
1026 an alternative mechanism for DNA cleavage activation. *Nucleic Acids Res.* **31**, 5449–5460  
1027 (2003).

1028 27. Guo, F., Gopaul, D. N. & van Duyne, G. D. Structure of Cre recombinase complexed  
1029 with DNA in a site-specific recombination synapse. *Nature* **389**, 40–6 (1997).

1030 28. Rongrong, L., Lixia, W. & Zhongping, L. Effect of deletion mutation on the  
1031 recombination activity of Cre recombinase. *Acta Biochim Pol* **52**, 541–4 (2005).

1032 29. Zoltowski, B. D., Vaccaro, B. & Crane, B. R. Mechanism-based tuning of a LOV  
1033 domain photoreceptor. *Nat Chem Biol* **5**, 827–34 (2009).

1034 30. Vaidya, A. T., Chen, C. H., Dunlap, J. C., Loros, J. J. & Crane, B. R. Structure of a  
1035 light-activated LOV protein dimer that regulates transcription. *Sci Signal* **4**, ra50 (2011).

1036 31. Guntas, G. *et al.* Engineering an improved light-induced dimer (iLID) for controlling  
1037 the localization and activity of signaling proteins. *Proc. Natl. Acad. Sci.* 201417910 (2014)  
1038 doi:10.1073/pnas.1417910112.

1039 32. Mata-Gómez, L. C., Montañez, J. C., Méndez-Zavala, A. & Aguilar, C. N.  
1040 Biotechnological production of carotenoids by yeasts: an overview. *Microb. Cell Factories*  
1041 **13**, 12 (2014).

1042 33. Verwaal, R. *et al.* High-Level Production of Beta-Carotene in *Saccharomyces*  
1043 *cerevisiae* by Successive Transformation with Carotenogenic Genes from *Xanthophyllomyces*  
1044 *dendrorhous*. *Appl. Environ. Microbiol.* **73**, 4342–4350 (2007).

1045 34. Asadollahi, M. A. *et al.* Production of plant sesquiterpenes in *Saccharomyces*  
1046 *cerevisiae*: Effect of ERG9 repression on sesquiterpene biosynthesis. *Biotechnol. Bioeng.* **99**,  
1047 666–677 (2008).

1048 35. Xie, W., Ye, L., Lv, X., Xu, H. & Yu, H. Sequential control of biosynthetic pathways  
1049 for balanced utilization of metabolic intermediates in *Saccharomyces cerevisiae*. *Metab. Eng.*  
1050 **28**, 8–18 (2015).

1051 36. Tippmann, S., Scalcinati, G., Siewers, V. & Nielsen, J. Production of farnesene and  
1052 santalene by *Saccharomyces cerevisiae* using fed-batch cultivations with RQ-controlled feed.  
1053 *Biotechnol. Bioeng.* **113**, 72–81 (2016).

1054 37. Fegueur, M., Richard, L., Charles, A. D. & Karst, F. Isolation and primary structure of  
1055 the ERG9 gene of *Saccharomyces cerevisiae* encoding squalene synthetase. *Curr. Genet.* **20**,  
1056 365–372 (1991).

1057 38. Link, K. H., Shi, Y. & Koh, J. T. Light activated recombination. *J Am Chem Soc* **127**,  
1058 13088–9 (2005).

1059 39. Sinha, D. K. *et al.* Photocontrol of protein activity in cultured cells and zebrafish with  
1060 one- and two-photon illumination. *Chembiochem* **11**, 653–63 (2010).

1061 40. Lu, X. *et al.* Optochemogenetics (OCG) Allows More Precise Control of Genetic  
1062 Engineering in Mice with CreER regulators. *Bioconjug. Chem.* **23**, 1945–1951 (2012).

1063 41. Luo, J. *et al.* Genetically encoded optical activation of DNA recombination in human

1064 cells. *Chem. Commun. Camb. Engl.* **52**, 8529–8532 (2016).

1065 42. Brown, W., Liu, J., Tsang, M. & Deiters, A. Cell-Lineage Tracing in Zebrafish

1066 Embryos with an Expanded Genetic Code. *ChemBioChem* **19**, 1244–1249 (2018).

1067 43. Morales, D. P. *et al.* Light-Triggered Genome Editing: Cre Recombinase Mediated

1068 Gene Editing with Near-Infrared Light. *Small* **14**, 1800543 (2018).

1069 44. Zhang, W. *et al.* Optogenetic control with a photocleavable protein, PhoCl. *Nat.*

1070 *Methods* **14**, 391–394 (2017).

1071 45. Morikawa, K. *et al.* Photoactivatable Cre recombinase 3.0 for in vivo mouse

1072 applications. *Nat. Commun.* **11**, 1–11 (2020).

1073 46. Takao, T. *et al.* Establishment of a tTA-dependent photoactivatable Cre recombinase

1074 knock-in mouse model for optogenetic genome engineering. *Biochem. Biophys. Res.*

1075 *Commun.* (2020) doi:10.1016/j.bbrc.2020.03.015.

1076 47. Allen, M. E. *et al.* An AND-Gated Drug and Photoactivatable Cre-loxP System for

1077 Spatiotemporal Control in Cell-Based Therapeutics. *ACS Synth. Biol.* **8**, 2359–2371 (2019).

1078 48. Wu, G. *et al.* Metabolic Burden: Cornerstones in Synthetic Biology and Metabolic

1079 Engineering Applications. *Trends Biotechnol.* **34**, 652–664 (2016).

1080 49. Verwaal, R. *et al.* Heterologous carotenoid production in *Saccharomyces cerevisiae*

1081 induces the pleiotropic drug resistance stress response. *Yeast* **27**, 983–998 (2010).

1082 50. Rest, M. E. van der *et al.* The plasma membrane of *Saccharomyces cerevisiae*:

1083 structure, function, and biogenesis. *Microbiol. Rev.* **59**, 304–322 (1995).

1084 51. Min, B. E., Hwang, H. G., Lim, H. G. & Jung, G. Y. Optimization of industrial

1085 microorganisms: recent advances in synthetic dynamic regulators. *J. Ind. Microbiol.*

1086 *Biotechnol.* **44**, 89–98 (2017).

1087 52. Solow, S. P., Sengbusch, J. & Laird, M. W. Heterologous Protein Production from the

1088 Inducible MET25 Promoter in *Saccharomyces cerevisiae*. *Biotechnol. Prog.* **21**, 617–620

1089 (2005).

1090 53. Møller, T. S. B. *et al.* Human  $\beta$ -defensin-2 production from *S. cerevisiae* using the

1091 repressible MET17 promoter. *Microb. Cell Factories* **16**, (2017).

1092 54. Kruijatz, F. *et al.* MicrOLED-photobioreactor: Design and characterization of a

1093 milliliter-scale Flat-Panel-Airlift-photobioreactor with optical process monitoring. *Algal Res.*

1094 **18**, 225–234 (2016).

1095 55. Hu, J.-Y. & Sato, T. A photobioreactor for microalgae cultivation with internal

1096 illumination considering flashing light effect and optimized light-source arrangement. *Energy*

1097 *Convers. Manag.* **133**, 558–565 (2017).

1098 56. Schreiber, C. *et al.* Growth of algal biomass in laboratory and in large-scale algal

1099 photobioreactors in the temperate climate of western Germany. *Bioresour. Technol.* **234**, 140–

1100 149 (2017).

1101 57. Zhao, E. M. *et al.* Optogenetic regulation of engineered cellular metabolism for

1102 microbial chemical production. *Nature* **555**, 683–687 (2018).

1103 58. Milias-Argeitis, A., Rullan, M., Aoki, S. K., Buchmann, P. & Khammash, M.

1104 Automated optogenetic feedback control for precise and robust regulation of gene expression

1105 and cell growth. *Nat. Commun.* **7**, ncomms12546 (2016).

1106 59. Zhuang, X. & Chappell, J. Building terpene production platforms in yeast. *Biotechnol.*

1107 *Bioeng.* **112**, 1854–1864 (2015).

1108 60. Yuan, J. & Ching, C.-B. Dynamic control of ERG9 expression for improved amorpha-

1109 4,11-diene production in *Saccharomyces cerevisiae*. *Microb. Cell Factories* **14**, 38 (2015).

1110 61. Peng, B. *et al.* A squalene synthase protein degradation method for improved

1111 sesquiterpene production in *Saccharomyces cerevisiae*. *Metab. Eng.* **39**, 209–219 (2017).

1112 62. Amiri, P., Shahpiri, A., Asadollahi, M. A., Momenbeik, F. & Partow, S. Metabolic

1113 engineering of *Saccharomyces cerevisiae* for linalool

1114 production. *Biotechnol. Lett.* **38**, 503–508 (2016).

1115 63. Paddon, C. J. *et al.* High-level semi-synthetic production of the potent antimalarial  
1116 artemisinin. *Nature* **496**, 528–532 (2013).

1117 64. Scalcinati, G. *et al.* Dynamic control of gene expression in *Saccharomyces cerevisiae*  
1118 engineered for the production of plant sesquiterpene  $\alpha$ -santalene in a fed-batch mode. *Metab.*  
1119 *Eng.* **14**, 91–103 (2012).

1120 65. Sadowski, I., Su, T. C. & Parent, J. Disintegrator vectors for single-copy yeast  
1121 chromosomal integration. *Yeast* **24**, 447–55 (2007).

1122 66. Laughery, M. F. *et al.* New Vectors for Simple and Streamlined CRISPR-Cas9  
1123 Genome Editing in *Saccharomyces cerevisiae*. *Yeast Chichester Engl.* **32**, 711–720 (2015).

1124 67. Yost, E. A., Mervine, S. M., Sabo, J. L., Hynes, T. R. & Berlot, C. H. Live Cell  
1125 Analysis of G Protein  $\beta 5$  Complex Formation, Function, and Targeting. *Mol. Pharmacol.* **72**,  
1126 812–825 (2007).

1127 68. Hermann, M. *et al.* Binary recombinase systems for high-resolution conditional  
1128 mutagenesis. *Nucleic Acids Res.* **42**, 3894–3907 (2014).

1129 69. Mangeot, P.-E., Cosset, F.-L., Colas, P. & Mikaelian, I. A universal transgene  
1130 silencing method based on RNA interference. *Nucleic Acids Res.* **32**, e102–e102 (2004).

1131 70. Hahne, F. *et al.* flowCore: a Bioconductor package for high throughput flow  
1132 cytometry. *BMC Bioinformatics* **10**, 106 (2009).

1133 71. Lee, J. *et al.* CHARMM-GUI Input Generator for NAMD, GROMACS, AMBER,  
1134 OpenMM, and CHARMM/OpenMM Simulations Using the CHARMM36 Additive Force  
1135 Field. *J. Chem. Theory Comput.* **12**, 405–413 (2016).

1136 72. Brooks, B. R. *et al.* CHARMM: The biomolecular simulation program. *J. Comput.*  
1137 *Chem.* **30**, 1545–1614 (2009).

1138 73. Humphrey, W., Dalke, A. & Schulten, K. VMD: Visual molecular dynamics. *J. Mol.*  
1139 *Graph.* **14**, 33–38 (1996).

1140 74. Haberthür, U. & Caflisch, A. FACTS: Fast analytical continuum treatment of  
1141 solvation. *J. Comput. Chem.* **29**, 701–715 (2008).

1142 75. Ryckaert, J.-P., Ciccotti, G. & Berendsen, H. J. C. Numerical integration of the  
1143 cartesian equations of motion of a system with constraints: molecular dynamics of n-alkanes.  
1144 *J. Comput. Phys.* **23**, 327–341 (1977).

1145 76. Torrie, G. M. & Valleau, J. P. Nonphysical sampling distributions in Monte Carlo  
1146 free-energy estimation: Umbrella sampling. *J. Comput. Phys.* **23**, 187–199 (1977).

1147 77. Kumar, S., Rosenberg, J. M., Bouzida, D., Swendsen, R. H. & Kollman, P. A. THE  
1148 weighted histogram analysis method for free-energy calculations on biomolecules. I. The  
1149 method. *J. Comput. Chem.* **13**, 1011–1021 (1992).

1150

1151 FIGURE LEGENDS

1152

1153

1154 **Figure 1. N-ter and C-ter  $\alpha$ -helices of Cre are critical for activity. a-b)** Structure of  
1155 the Cre tetramer complexed with DNA (PDB: 1NZB). The four N-ter domains (a) interact via  
1156 contacts between  $\alpha$ -helices A (green) and E (orange) and the four C-ter domains (b) interact  
1157 via  $\alpha$ -helices N (magenta). **c)** Yeast reporter system to quantify Cre efficiency. The STOP  
1158 element includes a selectable marker and a terminator sequence which prevents expression of  
1159 the downstream GFP sequence. **d)** Activity of wild-type and C-ter mutants of Cre measured  
1160 as the fraction of cells expressing GFP (mean +/- s.e.m,  $n = 3$  independent transformants).  
1161 Numbers denote the number of residues deleted from the C-ter extremity. 'Vect': expression  
1162 plasmid with no insert. **e)** Blow-up of  $\alpha$ N helix. **f)** Energetics of  $\alpha$ N displacing (see  
1163 methods). PMF: Potential of Mean Force ( $\pm$  error defined as  $\sigma_{F_i}$  in Methods). **g)** Activity of  
1164 Cre mutants lacking N-terminal residues 2 to X, combined or not with the A340 A341 C-  
1165 terminal mutation (mean +/- s.e.m,  $n = 3$  independent transformants). X was 21, 28 or 37 as  
1166 indicated. Arrows, significantly different from WT at  $p < 0.05$  (*t*-test). *ns*, non significant.  
1167

1168 **Figure 2. Monogenic LOV2-Cre fusions display photoactivatable recombinase**

1169 **activity. a)** Fusions with wild-type Cre. **b)** Variants of LOV2\_Cre32 carrying the indicated  
1170 mutations at the peptide junction. **c)** Fusion with Cre carrying the A340A341 double  
1171 mutation. **a - c)** Numbers indicate the positions on the Cre peptidic sequence where asLOV2  
1172 was fused. All bar plots show recombinase activity measured by flow-cytometry (mean  $\pm$  sem  
1173 of the proportion of switched cells,  $n = 5$  independent transformants) after galactose-induced  
1174 expression of the fusion protein, followed (cyan) or not (grey) by illumination at 460 nm, 36.3  
1175 mW/cm<sup>2</sup>, for 30 minutes. \*, \*\* and \*\*\*: significantly different between dark and light

1176 conditions at  $p < 0.05$ ,  $p < 0.01$  and  $p < 0.001$ , respectively (*t*-test). *n.s.*, non significant ( $p >$   
1177 0.05).

1178

1179 **Figure 3. Functional properties of LiCre. a-b)** Energy and time dependence. Yeast  
1180 cells carrying the reporter system of Fig. 1c and expressing LiCre were grown to stationary  
1181 phase and illuminated with blue light (460 nm, see methods) at indicated intensities, then  
1182 incubated in non-dividing conditions and processed by flow cytometry (mean  $\pm$  sem, strain  
1183 GY1761 transformed with pGY466);  $n = 4$  and 3 colonies in (a) and (b), respectively.

1184 Illumination conditions varied either in intensity (**a**) or duration (**b**). *p*: significance from *t*-  
1185 test ( $n=3$ ). The fraction of ON cells observed at 0 min was not significantly higher than the  
1186 fraction of ON GY1761 cells transformed with empty vector pRS314 ( $p>0.05$ ). **c)** Yeast strain  
1187 GY1761 was transformed with plasmids pGY491 and pGY501 to express the two proteins of  
1188 the nMag/pMag split Cre system of Kawano *et al.*<sup>21</sup>. Cells were processed as in (b) with a  
1189 light intensity that matched authors recommendations ( $1.815 \text{ mW/cm}^2$ ). Neg: no illumination,  
1190 cells containing empty vectors only. *p*: significance from *t*-tests ( $n= 4$ ). **d)** Yeast strain  
1191 GY1761 was transformed with plasmids pGY531 and pGY532 to express the two proteins of  
1192 the CRY2<sup>L348F</sup>/CIB1 split Cre system of Taslimi *et al.*<sup>20</sup>. Cells were processed as in (b) with  
1193 or without illumination for 90 min at an intensity matching authors recommendations ( $5.45$   
1194  $\text{mW/cm}^2$ ). Neg: no illumination, cells containing empty vectors only. **e)** Yeast cells  
1195 expressing LiCre from plasmid pGY466 and carrying an integrated reporter conferring  
1196 prototrophy to histidine were spotted on two His- plates at decreasing densities. Prior to  
1197 incubation at 30°C, one plate (right) was illuminated for 90 minutes at  $3.63 \text{ mW/cm}^2$   
1198 intensity. **f)** Time-lapse imaging of yeast cells expressing LiCre and carrying a similar  
1199 reporter as Fig. 1c but where GFP was replaced by mCherry (strain GY2033 with plasmid  
1200 pGY466). Cells were grown to stationary phase, illuminated for 90 min at  $3.63 \text{ mW/cm}^2$

1201 intensity, immobilized on bottom-glass wells in dividing condition and imaged at the  
1202 indicated time. Bar: 10  $\mu$ m. **g)** Quantification of intra-cellular mCherry fluorescence from (f),  
1203  $n = 22$  cells. **h)** Design of qPCR assay allowing to quantify recombination efficiency. **i)**  
1204 Quantification of excision by qPCR immediately after illumination at 3.63 mW/cm<sup>2</sup> intensity  
1205 (stationary phase, strain GY1761 transformed with pGY466). **j)** DNA excision does not occur  
1206 after illumination. X-axis: same data as shown on Y-axis in (i). Y-axis: same experiment but  
1207 after illumination, cells were incubated for 90 minutes in dark and non-dividing condition  
1208 prior to harvest and qPCR. **k)** Quantification of DNA excision by qPCR on exponentially-  
1209 growing or stationary-phase cells (strain GY1761 transformed with pGY466) illuminated at  
1210 3.63 mW/cm<sup>2</sup> intensity. Grey: no illumination. Bars in (i-k): s.e.m. ( $n=10$  colonies).

1211

1212 **Figure 4. Model of LiCre activation. a)** The model was built using PDB structures  
1213 1NZB (Cre) and 4WF0 (asLOV2). Green: residues of  $\alpha$ A helix from Cre. Blue: residues of J $\alpha$   
1214 helix from asLOV2. **b)** Two-colors switch assay. Yeast cells carrying LiCre and both GFP  
1215 and mCherry reporters (strain GY2214 with plasmid pGY466) were grown to stationary  
1216 phase in SD-M-W and illuminated for 180 min at 3.63 mW/cm<sup>2</sup> intensity. Cells were then  
1217 incubated in the dark in non-dividing conditions and processed by flow-cytometry. Density  
1218 plot (middle): fluorescent intensities for one sample. Barplot (right): mean  $\pm$  s.e.m. ( $n=3$   
1219 colonies) fraction of switched cells in the whole population (Green, Red, Red and green) or in  
1220 the subpopulation of cells that also switched the other reporter (Green among red, Red among  
1221 green). Grey bars: controls without illumination.

1222

1223 **Figure 5. Switching ON carotenoid production with light. a)**  $\beta$ -carotene  
1224 biosynthetic pathway. Exogenous genes from *X. dendrorhous* are printed in red. FPP,  
1225 farnesyl pyrophosphate; GGPP, geranylgeranyl pyrophosphate. **b)** Scheme of the switchable

1226 locus of yeast GY2247. **c)** Photoswitchable bioproduction. Strain GY2247 was transformed  
1227 with either pRS314 (Vect.), pGY466 (LiCre) or pGY502 (CreWT). Cells were cultured  
1228 overnight in SD-M-W and the cultures were illuminated (460 nm, 90 min, 36.3 mW/cm<sup>2</sup>) or  
1229 not and then spotted on agar plates. A and B correspond to two independent transformants of  
1230 the LiCre plasmid. Colonies on the right originate from the illuminated LiCre (A) culture. **d)**  
1231 Quantification of carotenoids production. Three colonies of strain GY2247 transformed with  
1232 LiCre plasmid pGY466 were cultured overnight in SD-W-M. The following day, 10 ml of  
1233 each culture were illuminated as in c), while another 10 ml was kept in the dark. These  
1234 cultures were then incubated for 72 h at 30°C. Cells were pelleted (colors of the cell pellets are  
1235 shown on picture) and processed for quantification (see methods). Units are micrograms of  
1236 total carotenoids per gram of biomass dry weight. Bars: mean +/- s.e.m, n = 3. **e)** Scheme of  
1237 the switchable locus of yeast GY2236. **f)** Light-induced deletion of squalene synthase gene.  
1238 Strain GY2236 was transformed with either pRS314 (Vect), pGY502 (Cre) or pGY466  
1239 (LiCre). Cells were cultured overnight in 4ml of SD-M-W. A 100-μl aliquot of each culture  
1240 was illuminated (as in c) while another 100-μl aliquot was kept in the dark. A dilution at ~1  
1241 cell/μl was then plated on SD-W. Colonies were counted after 3 days. *cfu*: colony forming  
1242 units (mean +/- sem, n ≥ 3 plates). \*\*: p<0.01 (t-test).  
1243

1244 **Figure 6. LiCre photoactivation in human cells. a)** Left: Lentiviral SIN vector for  
1245 LiCre expression (plasmid pGY577). *P<sub>CMV</sub>*, early cytomegalovirus promoter; SIN, LTR  
1246 regions of Simian Immunodeficiency Virus comprising a partially-deleted 3' U3 region  
1247 followed by the R and U5 regions; *psi*, retroviral psi RNA packaging element; *cPPT* and *PPT*,  
1248 central and 3' polypyrimidine tracks, respectively; *RRE*, Rev/Rev-responsive element; *SA*, SIV  
1249 Rev/Tat splice acceptor; *NLS*, nuclear localization signal; *WPRE*, woodchuck hepatitis virus  
1250 regulatory element; *Helper*, plasmid coding for *gag*, *pol*, *tat* and *rev*; *VSV-g*, plasmid

1251 encoding the envelope of the vesicular stomatitis virus. Co-transfection in HEK293T cells  
1252 produces pseudotyped particles. These particles are deposited on T4-2PURE reporter cells  
1253 which are then illuminated and imaged. Right, genomic reporter locus of T4-2PURE cells.  
1254  $P_{SV40}$ , Promoter from SV40; *FRT*, FLP recognition targets;  $Hyg^R$ , hygromycin resistance; *pA*,  
1255 poly-adenylation signal from SV40;  $Zeo^R$ , zeomycin resistance. Recombination between LoxP  
1256 sites switches ON the expression of mCherry by removing three pA terminators. **b)**  
1257 Microscopy images of T4-2PURE cells following the assay. Bars, 150  $\mu$ m. All three  
1258 fluorescent frames were acquired at the same intensity and exposure time. Illumination  
1259 corresponded to two 20 min exposures at 3.63 mW/cm<sup>2</sup>, separated by 20 minutes without  
1260 illumination.

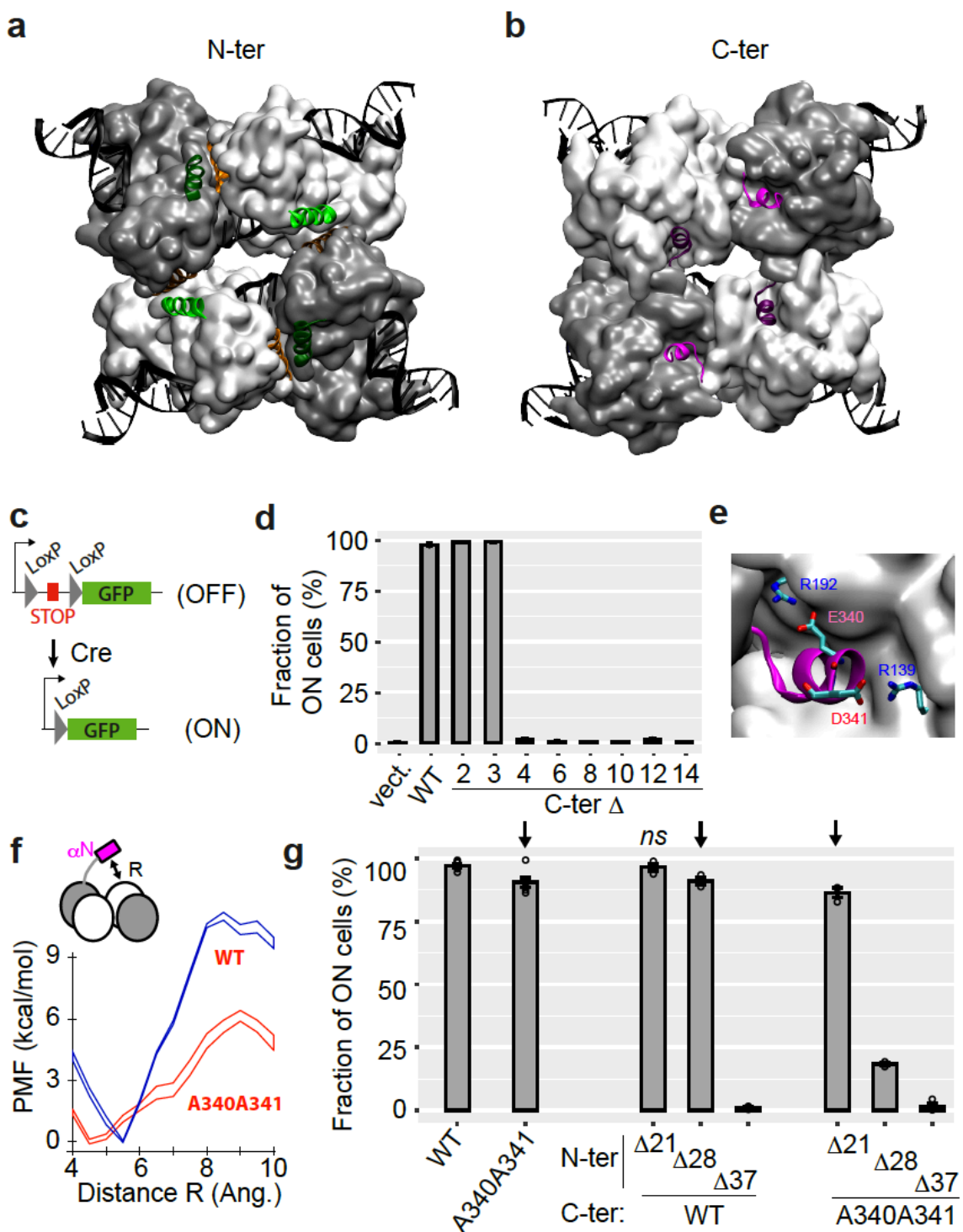
1261

1262

1263

1264

Figure 1

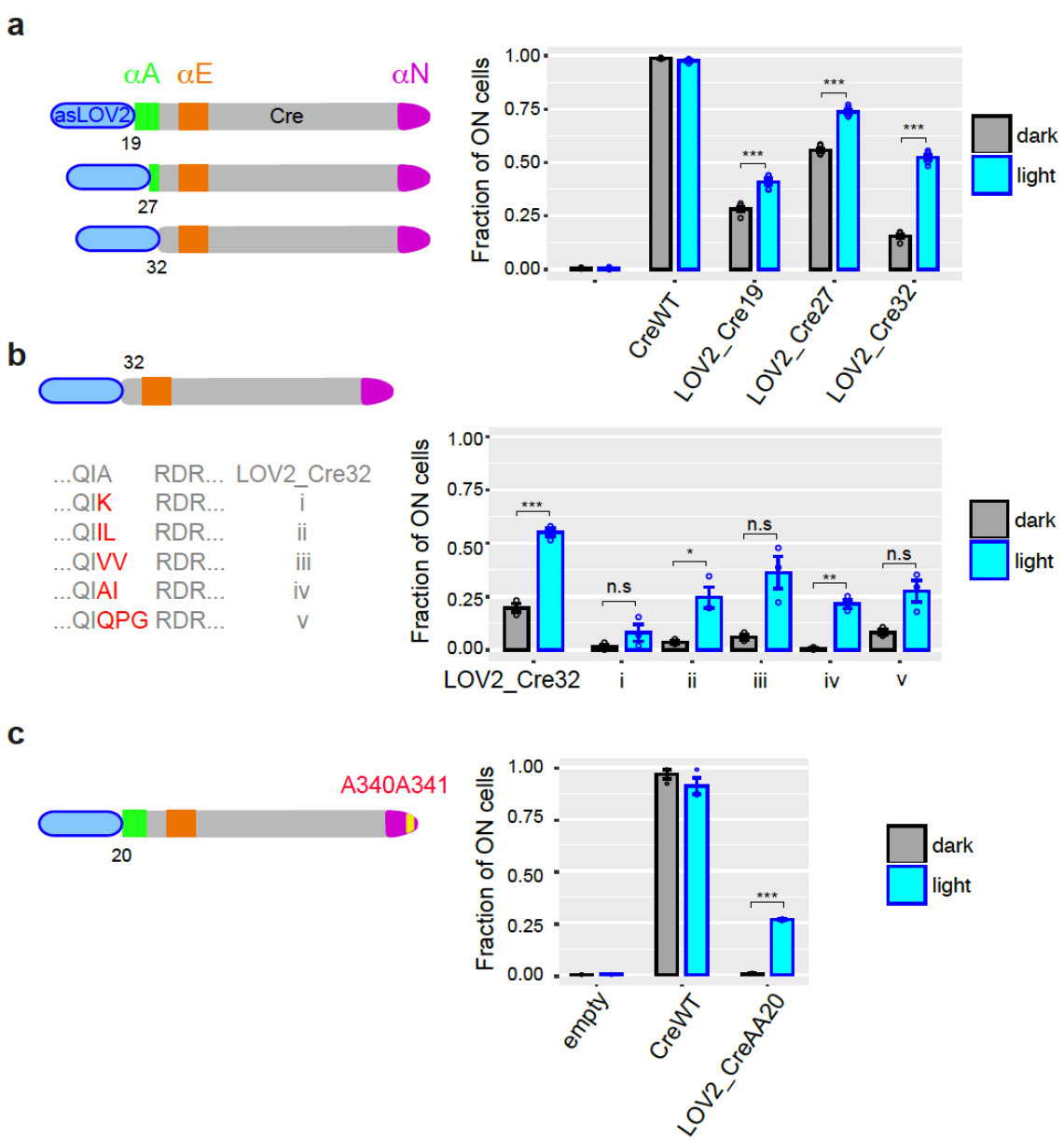


1265

1266

1267

Figure 2

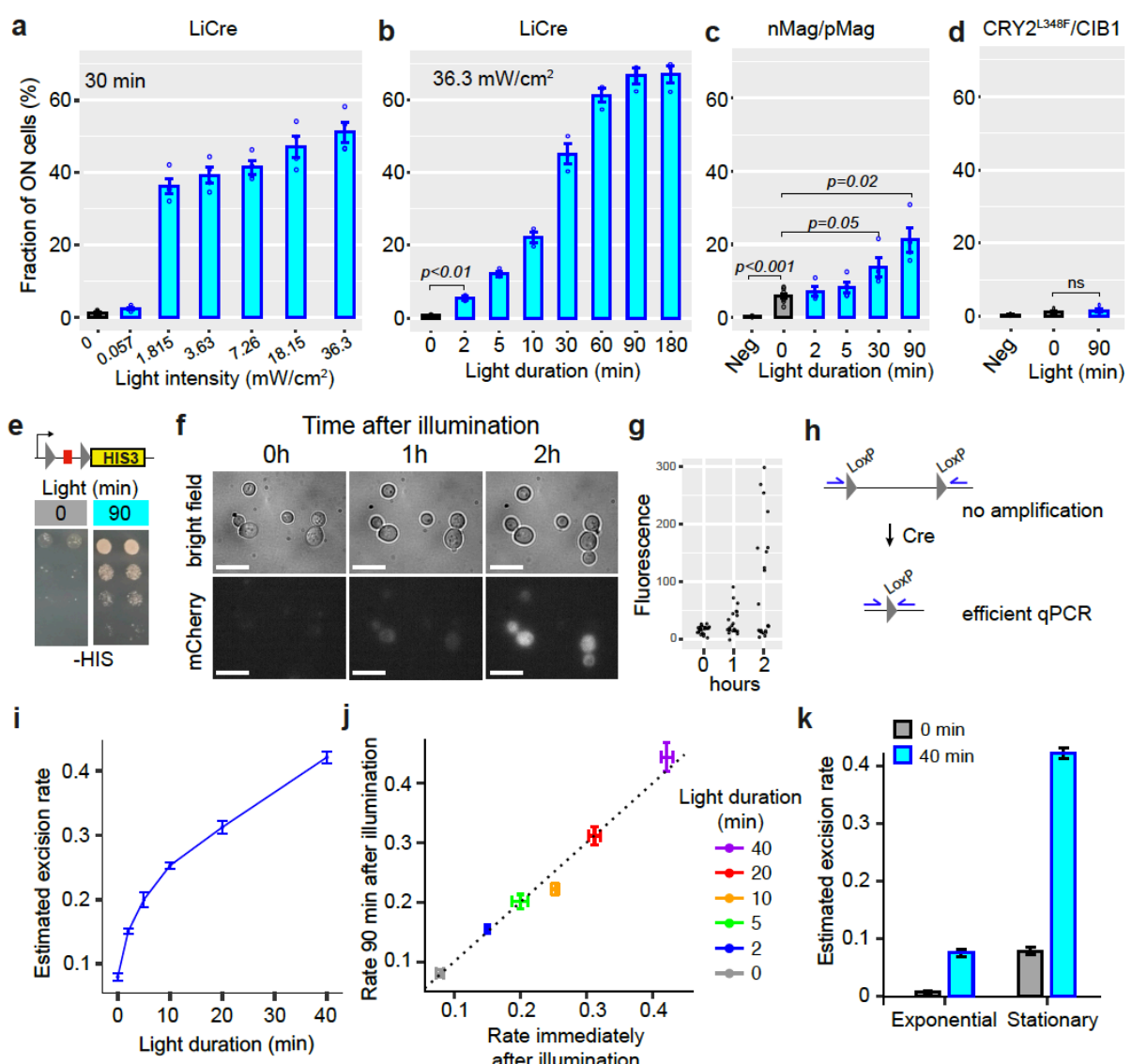


1268

1269

1270

Figure 3

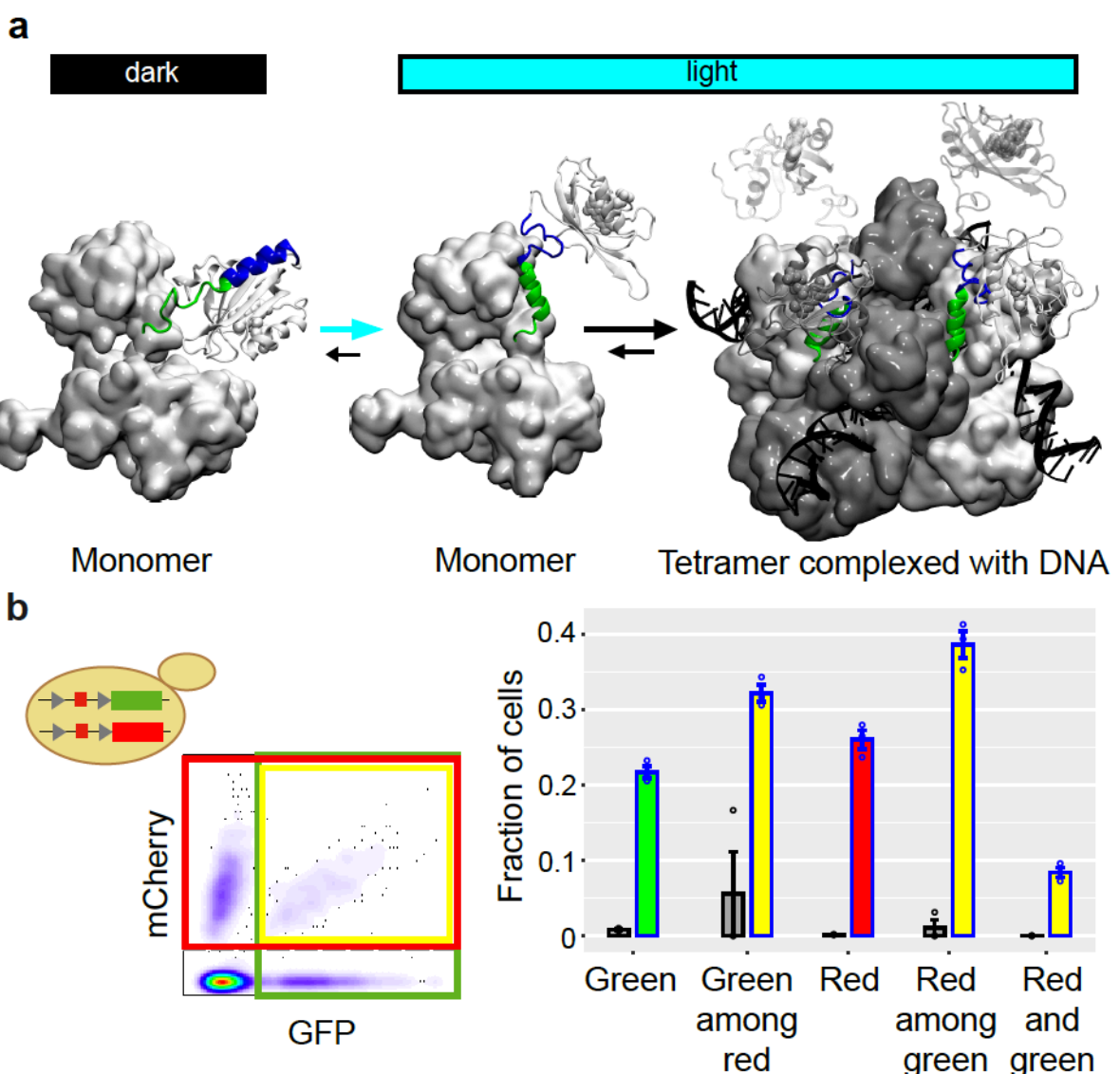


1271

1272

1273

Figure 4



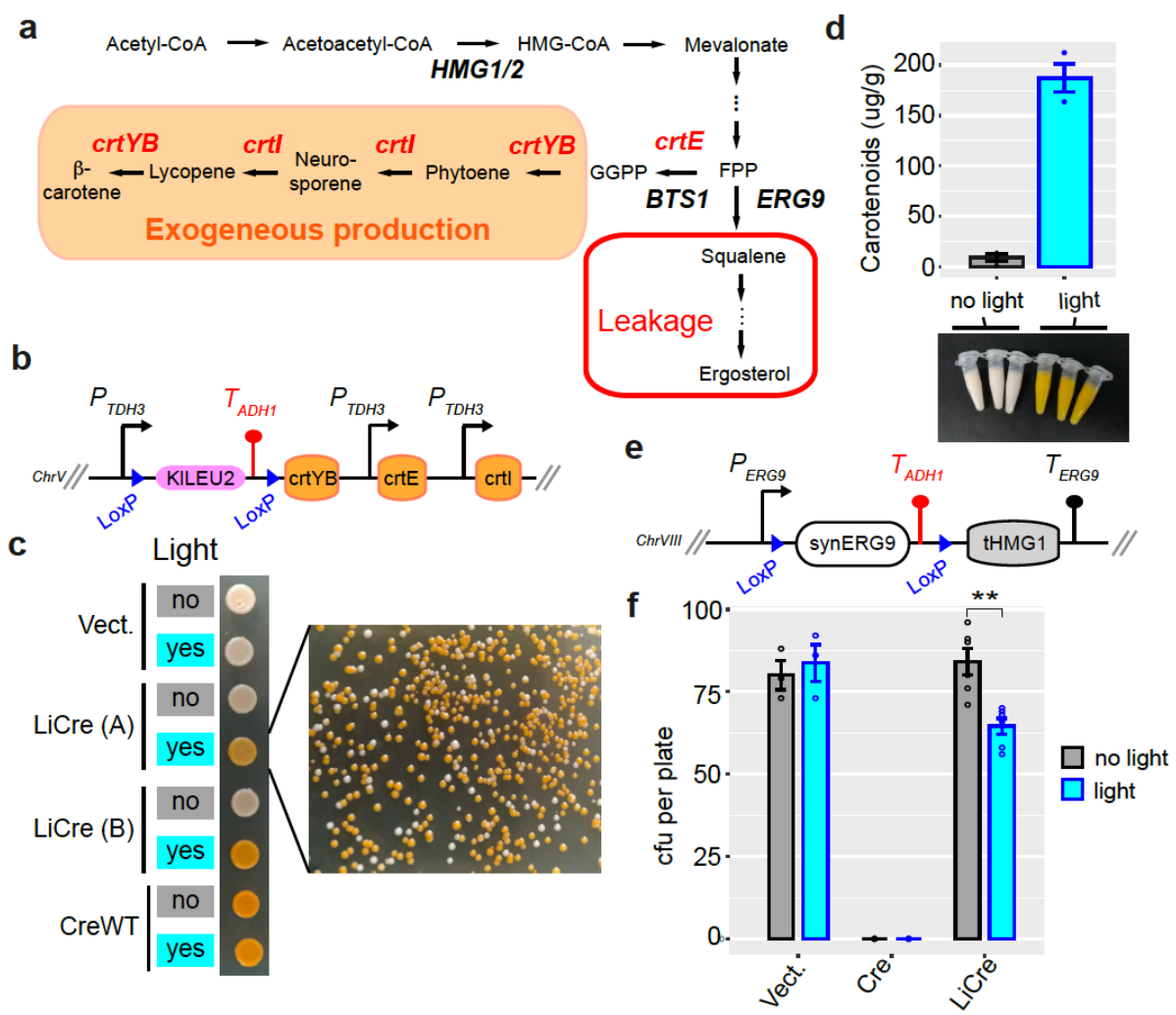
1274

1275

1276

1277

Figure 5

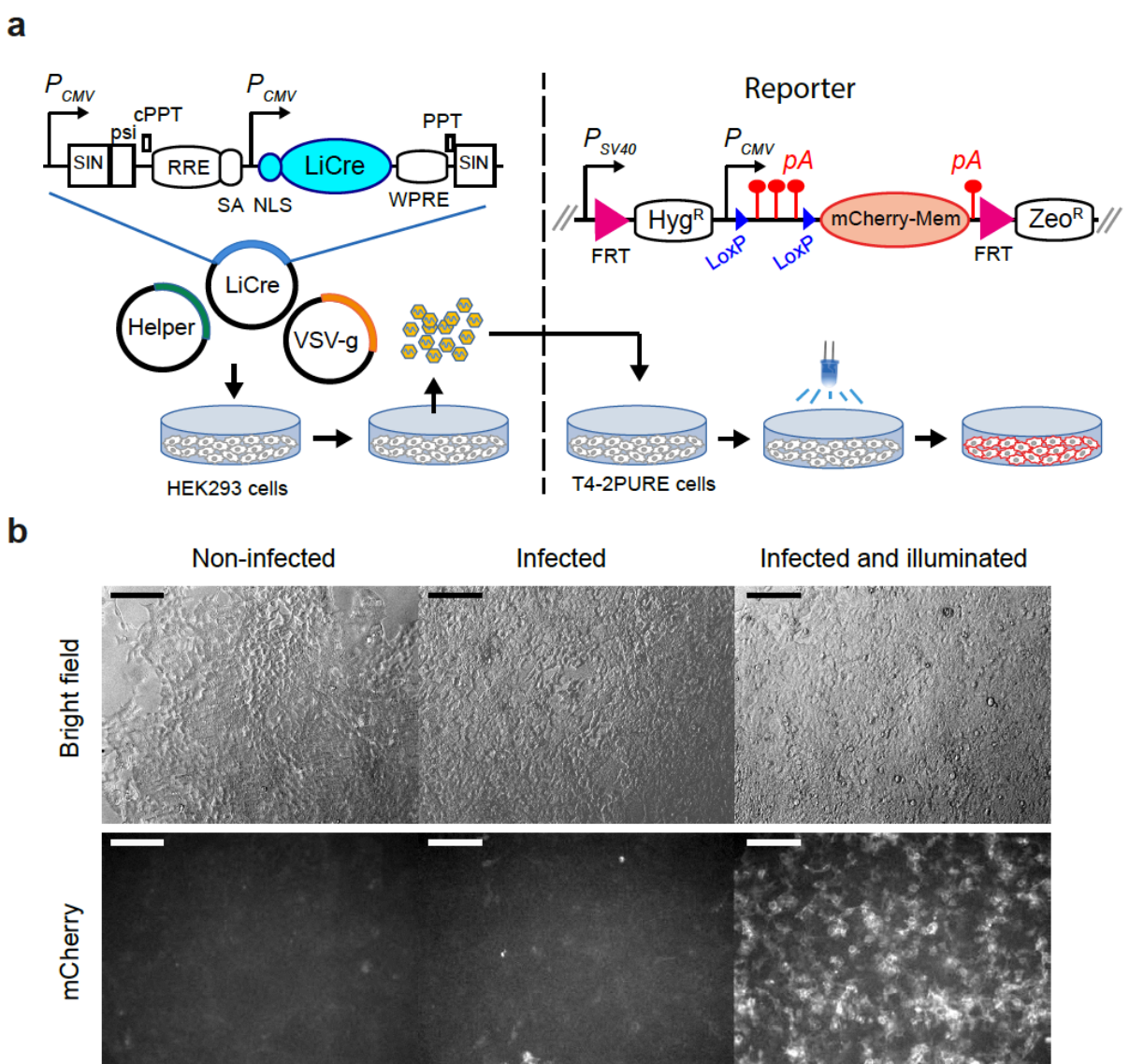


1278

1279

1280

Figure 6



1281

1282